

**Using mark-recapture models to understand goose-beaked whale
residency in Southern California**

David A. Sweeney

A thesis submitted for requirements for the degree of
Master of Science in Statistics



**University of
St Andrews**

School of Mathematics and Statistics

Table of Contents

1 Abstract	2
2 Introduction	2
3 Methods	5
3.1 Data collection	5
3.1.1 Photo-identification data	5
3.1.2 Tag data	6
3.2 Model structure	8
3.2.1 Complete data likelihood	10
3.2.2 Marginalised likelihood	10
3.3 Simulations	11
3.4 Case study: Goose-beaked whales	12
4 Results	13
4.1 Simulations	13
4.2 Case study: Goose-beaked whales	14
5 Discussion	19
6 Acknowledgements	24
6.1 Funding	24
6.2 Data ethics and availability	24
6.3 Declaration statement	25
7 References	25

1 Abstract

Goose-beaked whales (*Ziphius cavirostris*) are of global conservation interest given observed behavioural responses and occasional strandings in response to anthropogenic noise. A resident population exists in Southern California that heavily overlaps with a US Navy training range. A long-term research project exists to monitor goose-beaked whale population dynamics possibly changing as a result of frequent exposure to sonar. Mark-recapture models for this population have previously hypothesized that transient individuals from a broader Pacific metapopulation may be biasing estimates of resident abundance and population dynamics. Therefore, we developed a continuous-time open-population mark-recapture model that accounts for a mixture of residents and transients within the study population. Using a marginalised likelihood and a multi-state framework extended from the Schwarz and Arnason model, we showed that a subset of captured goose-beaked whales in Southern California exhibit lower apparent survival due to a transience effect, thus allowing for differentiation between residency states. Results show possible resident population growth over the course of the study, although it cannot be ruled out that Southern California may be acting as an “ecological trap”, whereby residents might be dying off while simultaneously being replaced at a higher rate by immigrating and breeding transients from the metapopulation. Despite promising advancements in understanding local goose-beaked whale population dynamics, low detection probabilities and the short time window during which transients are predicted to be available for capture relative to the field survey sampling regime hinder precise estimation of transient entry and apparent mortality rates. Evidence was also found, with the aid of tag data, suggesting emigration and re-immigration are common, even with resident whales, thus negatively biasing detection probability. Such movement patterns question the efficacy of categorizing whales as resident or transient rather than viewing residency on a continuum where whales inhabit Southern California waters more or less frequently. Improved understanding of goose-beaked whale residency patterns will help explain variation in sonar responses observed, which in turn will inform models of long-term aggregate sonar exposure levels. Ultimately, an improved understanding of population structure will enhance population consequences of disturbance models that can forecast effects of changing sonar regimes on population dynamics.

2 Introduction

Goose-beaked whales (*Ziphius cavirostris*; also known as Cuvier’s beaked whales, Rogers et al., 2024) are cosmopolitan and are considered the most widely distributed beaked whale species (Macleod et al., 2005). In general, beaked whales are a family of marine mammals specially adapted for deep diving and poorly understood, given that some species were never observed alive in the wild until just recently (Pabst et al., 2016; Henderson et al., 2025). Available records suggest that goose-beaked whales are the deepest and longest diving animal on the planet, and they use echolocation to find prey at depth (Johnson et al., 2004; Auster and Watling, 2009; Quick et al., 2020; Visser et al., 2021; Coates et al., 2024). Following deep and long foraging dives, these whales typically perform a series of shallower non-foraging dives, and all dives are interspersed by surfacing periods often lasting less than 3 minutes (Baird et al., 2006; Tyack et al., 2006; Schorr et al., 2014; Shearer et al., 2019). These behaviour patterns cause them to be a highly elusive, yet fascinating study species.

Despite being listed as a species of “least concern” by the International Union for Conservation of Nature and Natural Resources (Robert Brownell Jr et al., 2020), goose-beaked whales are of global conservation

interest given their observed sensitivities to anthropogenic noise (Cox et al., 2006; Feyrer et al., 2024). Although perhaps most famously known for behavioural responses and occasional strandings in association with naval sonar activity around the world (DeRuiter et al., 2013; Falcone et al., 2017; Bernaldo De Quirós et al., 2019), these whales have also been shown to respond to other anthropogenic noises. Aguilar Soto et al. (2006) presented a case of reduced foraging effort from a goose-beaked whale in the Ligurian Sea coincident with the passage of a nearby vessel. Trickey et al. (2022) showed reduced vocal presence of these whales around Guadalupe Island, México in response to ultrasonic antifouling devices. Commercial echosounders have also been linked to decreased beaked whale acoustic detections in the western North Atlantic (Cholewiak et al., 2017). Anecdotal evidence suggests goose-beaked whales in Southern California may also alter behaviours in responses to some explosive sounds (Sweeney et al., 2022). In the context of strandings, theories explaining the pathology of sound-induced mortality are continually advancing (Fahlman et al., 2014, 2021; Fahlman, 2023). Meanwhile, long-term research projects monitor for changing population dynamics as a result of frequent exposure to acoustic stressors (Hooker et al., 2019).

The Southern California Anti-submarine Warfare Range (SOAR) is one of the most active sonar training ranges in the world. Thanks to the US Navy's Marine Mammal Monitoring on Navy Ranges (M3R) system (Jarvis et al., 2014), which uses real-time vocal detections to help field biologists locate elusive beaked whales for research purposes, collaborative research shows goose-beaked whales are found year-round in relatively high density (lower density in summer months) within SOAR and the surrounding waters of the San Nicolas Basin despite their known sensitivities to anthropogenic noise (Schoenbeck et al., 2024; Curtis et al., 2020). There has never been a definitive link made between sonar activity and strandings of goose-beaked whales in Southern California (Filadelfo et al., 2009; Adams et al., 2015; West et al., 2017), although it remains possible that sonar exercises have caused rare mortality without it being detected (Faerber and Baird, 2010; Moore et al., 2020; Peltier et al., 2025). Such disturbances have been inferred to reduce individual fitness in marine mammals if frequently occurring for extended periods of time (New et al., 2013; Siegal et al., 2022; Hin et al., 2023; Pirotta et al., 2022a). Despite the risks of inhabiting SOAR due to anthropogenic disturbance, tag recordings of movement and diving behaviour and prey density estimates reveal SOAR to be favourable foraging habitat for this species (Southall et al., 2019; Coates et al., 2024). Ongoing monitoring of goose-beaked whale abundance, survival, and population change around SOAR allows assessments into whether acute disturbance from sonar and combined effects with other stressors are impacting population health over time (Pirotta et al., 2018; Czapanskiy et al., 2021; Joy et al., 2022; Pirotta et al., 2022a; Tyack et al., 2022).

Estimates of beaked whale occurrence, density and abundance have been obtained using a variety of survey and analytical methods. Occurrence has historically been monitored via a combination of live-sighting and stranding information (Macleod et al., 2005), and more recently, via environmental DNA (Boldrocchi et al., 2024). Spatio-temporal trends in relative abundance and density have been assessed via continuously-recording, bottom-mounted hydrophones (Baumann-Pickering et al., 2014; Fregosi et al., 2020; Schoenbeck et al., 2024). Abundance has been estimated using visual line transect distance sampling surveys from vessels and aerial survey platforms (McLellan et al., 2018; Fiedler et al., 2023). However, the elusive behaviour of beaked whales, weather conditions, and vessel/aircraft speed likely result in a large proportion of missed detections during visual line transect surveys (Barlow et al., 2006; Barlow, 2015). For this reason, and given beaked whales' reliance on echolocation to forage (Johnson et al., 2004; Zimmer et al., 2005), abundance and density have also been estimated via point transect surveys with drifting acoustic recording systems and via bottom-mounted hydrophone arrays and cue counting techniques that combine acoustic density data

with group size estimates from vessel surveys (Marques et al., 2009; Moretti et al., 2010; Barlow et al., 2022). Finally, mark-recapture methods have been used, notably in Southern California, where a long-term goose-beaked whale monitoring project exists, in part, to monitor abundance by tracking individual animals through time (Curtis et al., 2020).

Mark-recapture (or capture-recapture) studies involve observations of distinct individuals over time to generate individual “capture” histories (King and McCrea, 2019). At the time an individual is first observed, that individual is uniquely “marked” (either by application of a distinguishing tag/ring or by recording natural markings that can be used to differentiate individuals). Subsequent observations of the individual are then termed “recaptures”. Mark-recapture data can be summarized into a binary matrix where each row represents a unique individual, each column represents a sampling occasion, and each element in the matrix can be either 1 or 0 depending on whether the individual was observed on the given sampling occasion. While different analytical approaches exist to model mark-recapture data with different underlying assumptions and research objectives, here we focus on open-population models, with particular emphasis on those deriving from the Jolly-Seber model (Jolly, 1965; Seber, 1965; Seber and Schofield, 2019). Open-population models allow for population gains (birth and immigration) and losses (death and emigration) between sampling occasions (Murray and Sandercock, 2019). Within sampling occasions, however, it is assumed there are no gains or losses, thus requiring sampling occasions to be short relative to the rate at which demographic processes occur. The Jolly-Seber model assumes equal probability of capture for both marked and unmarked individuals, thus allowing complete capture histories (including periods before first capture) to inform estimates of apparent survival (death or permanent emigration), entry (birth or immigration), abundance, and encounter probability (to account for imperfect detection of individuals during sampling occasions). When summarised into regularly spaced, discrete sampling periods (e.g., seasonal sampling occasions), population gains and losses can be modelled as probabilities of an individual entering or leaving the population across the interval between occasions. Continuous-time models, on the other hand, facilitate modelling of irregularly-spaced sampling periods, where demographic processes are modelled via (constant or varying) rates per unit of time (Hwang and Chao, 2002; Fouchet et al., 2016; Rushing, 2023). Whether using a discrete- or continuous-time model, accurate inference requires extended monitoring to gather sufficient records of new entrants, departures, and repeat encounters with previously marked individuals.

Given the elusive nature of goose-beaked whales and the need to generate a sufficient time series of captures, mark-recapture analysis was not feasible for estimating abundance, survival, and population change in Southern California until recently. Curtis et al. (2020) used 11 years (2007 – 2018) of goose-beaked whale photo-identifications in the San Nicolas Basin, with individual capture histories spanning 1 day to 11 years. These data were collected using pictures of individuals’ natural markings (e.g., scars, pigmentation, and dorsal-fin shape) from small-boat surveys (more detail in Section 3.1.1). Relevant to the current study, Curtis et al. highlighted that additional years of data would reduce uncertainty in estimates of population change and that several lines of evidence point to the presence of transient goose-beaked whales that pass through SOAR (Curtis et al., 2020). Individual variation in foraging behaviour and movement patterns provide further evidence to the presence of transient whales moving through SOAR (Barlow et al., 2020; Coates et al., 2024). Similar analyses for goose-beaked whales in the Ligurian Sea suggested variation in annual population growth was largely explained by immigration (Tenan et al., 2023). This analysis did not account for any transience effect or model emigration, however, thus confounding whether “immigration” was truly recruitment or the influx of transient individuals from other subpopulations in the Mediterranean Sea (Podesta et al., 2006; Onoufriou et al., 2022).

Within mark-recapture analyses, the transience effect refers to a lower-than-expected recapture of certain individuals due to biological factors or features of the sampling procedure (Genovart and Pradel, 2019; Oro and Doak, 2020). Transience can be caused by age or reproductive effects, whereby older individuals or first-time reproducers may have higher mortality than younger individuals or individuals that have experience reproducing (Genovart and Pradel, 2019). Transience can also be linked to dispersal, either for reproductive purposes or due to, for example, deteriorating habitats (Oro and Doak, 2020). Mark-recapture analyses of marine mammal populations typically define transients as individuals belonging to a larger metapopulation that are only sighted once (or relatively few times) during the study (Silva et al., 2009; Conn et al., 2011; Fearnbach et al., 2012; Madon et al., 2013; Haughey et al., 2020; Somerford et al., 2022). When unaccounted for, the transience effect can bias model estimation. For example, when primarily interested in resident population dynamics, the transience effect can cause overestimation of resident abundance and entry probability while also causing underestimation of detection and survival probabilities. Given concerns over biased estimation, accounting for transients is a common endeavour whenever possible in mark-recapture analyses Sasso et al. (2006); Belda et al. (2007); Choquet et al. (2017); Telenský et al. (2024), and it is the driving purpose behind this study.

In the context of goose-beaked whales at SOAR, differentiating between residents and transients enhances monitoring of the resident population over time. It also allows investigations of different sonar exposure rates and behavioural responses (e.g., if resident whales habituate to sonar, thus reducing response severity), which in turn can inform separate estimations of long-term aggregate sonar exposure levels for residents and transients (Joy et al., 2022). Accounting for transients can also greatly improve estimates of vital rates (e.g., reproductive rates) in multi-state mark-recapture models where individuals can transition between different age classes and new individuals can enter the population via a birth process (Tenan et al., 2023). All these enhancements can later be incorporated into population consequence of disturbance (PCoD) models, where disturbance-induced behavioural and physiological changes accumulate to affect individuals' health and vital rates, which are then integrated over all individuals in the population to predict effects on population dynamics (Pirotta et al., 2022a,b). In the context of goose-beaked whales, PCoD models have been used to predict consequences of changing sonar regimes (Moretti et al., 2018; Hin et al., 2023).

This study presents a Bayesian, continuous-time, open-population, mark-recapture model applied to goose-beaked whales in Southern California that distinguishes between residents and transients to update estimates of abundance from Curtis et al. (2020). Simulations are used to quantify uncertainty in the estimation of parameters given limitations of the goose-beaked whale sampling regime (see Section 3.1. We discuss the relevance of the results for goose-beaked whale population monitoring, while also acknowledging limitations of this study. Finally, we highlight future directions given the long-term objective of understanding how differential residency can inform models of goose-beaked whale population consequences of sonar disturbance in Southern California.

3 Methods

3.1 Data collection

3.1.1 Photo-identification data

Photo-identification data collection and processing were undertaken prior to the commencement of this study (see Section 6.2 for information on data ethics and availability). Photo-identification data of goose-

beaked whales were collected in the Southern California Bight from August 2006 through January 2025 on a highly irregular schedule. Most sightings occurred from 5-7 m rigid-hull inflatable boats (RHIBs) within the San Nicolas Basin. When operating in the San Nicolas Basin from October 2007 onward, surveys usually involved collaboration between vessel crew and passive acoustic observers from the M3R team, who monitored the approximately 1800-sq-km hydrophone array within SOAR and directed vessels to areas of detected beaked whale vocalizations. We hereafter refer to such days of survey effort on RHIBs in the San Nicolas Basin after October 2007 as “directed effort”. Directed effort usually consisted of a series of consecutive survey days over the course of 1-2 weeks; the median number of days between days of directed effort was 1, but the mean and maximum gap was 20.41 and 334 days, respectively. Additional sightings occurred opportunistically throughout the study period, either during field efforts with differing research protocols/objectives or from citizen scientists (e.g., whale watch boats). Photo-identification data processing followed the methods detailed in (Curtis et al., 2020).

Similar to previous mark-recapture analyses for this population (Curtis et al., 2020; Falcone et al., 2025), photo-identification data were filtered prior to modelling. We only modelled sightings from directed effort with known weather conditions within the San Nicolas Basin (Figure 1). We excluded calves given that (unmodelled) associations between a mother and calf violate the standard mark-recapture model assumption that captures are independent. Finally, we only modelled right- or both-sided captures (left-side only captures were slightly less prevalent) to prevent inflation of abundance estimates when not accounting for unknown links between left- and right-side captures (McClintock et al., 2013). All identifications excluded from modelling are hereafter referred to as “supplementary”.

3.1.2 Tag data

Tag data were collected prior to the commencement of this study (see Data ethics and availability: 6.2) and were used for purposes of model validation. Satellite transmitters anchored to the body of whales (i.e., Type A tags as per Andrews et al., 2019; hereafter “tags”) were developed by Wildlife Computers Inc. and deployed on goose-beaked whales in the Southern California Bight from August 2008 through January 2025. Tag deployments occurred from RHIBs via two different methods depending on the type and size of the tag. Smaller tags (Spot5, Mk10-A, and SPLASH10-F) were deployed in the Low Impact Minimally Percutaneous External-electronics Transmitter (LIMPET) configuration via a modified air rifle. Larger tags (Lander 2 and SMRT) were placed onto whales via a carbon-fibre pole. All tags recorded and transmitted Argos and/or GPS position estimates via satellite. Further details on tag specifications and deployment methods are available (Schorr et al., 2014; Barlow et al., 2020; Sweeney et al., 2022).

As part of this project, GPS locations were filtered to remove locations with residuals > 35 and time errors > 3 min (Dujon et al., 2014). Retained GPS, deployment (obtained manually), and Argos locations were then combined and manually assessed to identify and remove extraordinarily erroneous GPS location estimates and Argos location estimates with location class 2 or 3. Retained locations were then processed using the Douglas Argos Filter’s (Douglas et al., 2012) distance-angle-rate method (custom R implementation on GitHub: WCtagproc) with filtering parameters as follows: maximum redundant distance of 3 km, sustainable movement rate of 10 km/hr, turn angle tolerance coefficient of 25, rate filtering only, and Argos location class threshold of 2. For deployment and GPS locations to pass through and enhance precision of the Douglas Argos Filter, these location estimates were assigned to Argos location class 3. See Dujon et al. (2014) and McClintock et al. (2015) for more details on the accuracy of Argos and GPS tag position estimates.

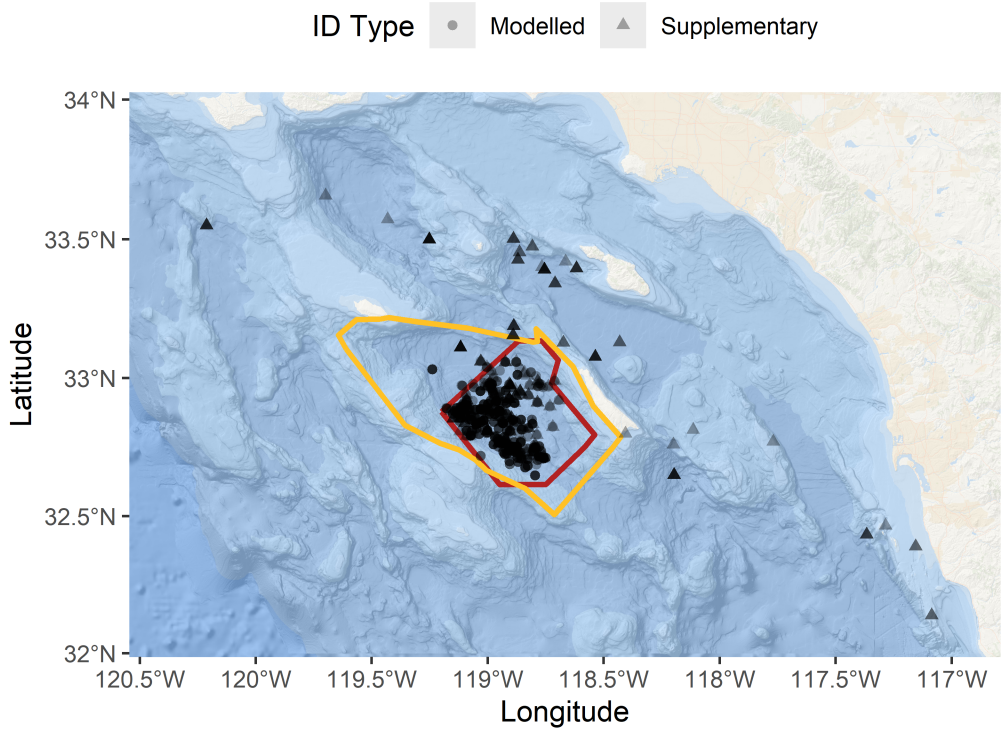


Figure 1: Map of goose-beaked whale sighting locations in the Southern California Bight. Points are shaped based on whether they were included in mark-recapture modelling (see Section 3.4 for data filtering details) or whether they were supplementary sightings for qualitative investigations. The San Nicolas Basin (gold) and Southern California Anti-submarine Warfare Range (SOAR; red) are also shown as polygons encompassing the bulk of whale sightings given directed effort in the region. For reference, the map is oriented such that north is upwards, the thin island bordering the eastern edge of the San Nicolas Bain is San Clemente Island, and Los Angeles, California is near the peninsula to the northeast of SOAR.

3.2 Model structure

We developed an open-population model that accounts for a mixture of residents and transients within the population. The model was designed with Southern California goose-beaked whales in mind, but it is generalizable to other study populations. Given irregularity in the spread of survey days during this study and uncertainty regarding the seasonality of demographic processes in goose-beaked whales in Southern California, entry and survival probabilities were handled in continuous time as a function of time between days of directed effort (hereafter called sampling occasions) and constant entry and mortality rates. The continuous-time parametrization also allowed all sampling occasions to contribute to model estimation and minimized bias due to violations of demographic closure in previous mark-recapture analysis that discretized sightings into annual time bins (Curtis et al., 2020). Detection was treated as a discrete, daily process during each sampling occasion, and captures were assumed instantaneous.

We opted for a custom Bayesian implementation of the model for a variety of reasons. To the best of our knowledge, there is no existing code that implements the desired model framework. Also, Bayesian methods allow posterior distributions to reflect uncertainty more naturally without assumptions of asymptotic normality. As detailed below, hard bounds on prior distributions also enable efficient separation of resident and transient apparent survival. Straightforward estimation of derived quantities and associated uncertainty via Mark chain Monte Carlo sampling was also desirable. Finally, custom model implementation provided flexibility when new parametrizations were required.

We developed two different parametrizations of the open-population model. Our first model parametrization used a complete data likelihood (see Section 3.2.1) to allow the model to be structured hierarchically as a state-space model via data augmentation (Tanner and Wong, 1987; Gimenez et al., 2007; Schofield et al., 2009). Under this framework, the model can be structured as a multi-state model whereby entry and removal processes transition individuals between states over time (Kéry and Schaub, 2012). Under data augmentation with a “superpopulation” of size M , abundance estimation involves estimating the states of putative individuals and counting entered and alive (resident and transient) individuals at each sampling occasion. Thus, whether an individual has entered and is alive and whether that individual is a resident or transient are both latent states to be estimated. Under data augmentation, the value for M is arbitrarily chosen, and the superpopulation is constructed by adding $M - n$ unobserved capture histories (where n is the number of observed individuals). However, M must be substantially greater than the maximum possible number of existing individuals during the study, regardless of whether or not they were detected, otherwise parameter estimation will be biased (Kéry and Schaub, 2012). The complete data likelihood framework removes the need for complex integration when expressing the likelihood function, but it can easily become computationally intensive and place extreme demands on computer memory given the large number of latent states being estimated for each individual across all sampling occasions in our continuous-time context.

Given computational issues when initially attempting to fit the complete data likelihood framework to data, we developed a marginalised likelihood approach that sums over all possible latent state sequences (see Section 3.2.2). Our marginalised likelihood approach was based on what is commonly referred to as the Schwarz and Arnason model (Schwarz and Arnason, 1996), which is structured using a binomial expression accounting for the likelihood contribution of both observed and unobserved individuals. In addition to no longer sampling each latent state, another notable difference compared to the complete data likelihood method is that the marginalised likelihood obviates the need for data augmentation in order to estimate abundance. Rather, the Schwarz and Arnason model includes an abundance parameter in the likelihood function and assumes all individuals in the population enter and are available for capture during the study

period. Following King and McCrea (2019), the likelihood function is expressed as:

$$L(N, \mathbf{x}, n, \boldsymbol{\theta}) = \binom{N}{n} \Pr(\mathbf{x}_0 | \boldsymbol{\theta})^{N-n} \prod_{i=1}^n \Pr(\mathbf{x}_i | \boldsymbol{\theta}), \quad (1)$$

where N is the estimated total number of residents and transients that entered the population and were thus available for capture during the study, n is the number of observed individuals, x_i represents the capture history of the i th observed individual, x_0 represents the capture history of an individual that was never observed, and $\boldsymbol{\theta}$ is a parameter vector containing parameters related to assigning individuals as residents or transients as well as entry, survival, and detection probabilities. The initial component of Equation 1 is the combinatorial binomial coefficient, which ensures the likelihood reflects the probability of observing a set of n individuals from N .

In Sections 3.2.1 and 3.2.2, we detail the different parametrizations of the complete data and marginalised likelihoods. For consistency and clarity in presenting each method, we present both likelihoods using a multi-state framework, where each animal can be in one of 4 possible k states across O sampling occasions: (1) not entered into the marked population, (2) entered as a resident and alive, (3) entered as a transient and alive, or (4) “apparently” dead (i.e., either dead or permanently left the study area). Individuals can only be detected while in states 2 and 4 (i.e., when entered and alive).

Across both formulations, we define ω as the proportion of individuals present on the first sampling occasion ($o = 1$), and ξ as the probability that initially present individuals were residents. $\boldsymbol{\pi}$ is the initial state occupancy probabilities, where π_k is the probability an individual was in state k during the first sampling occasion. $\boldsymbol{\pi} = (1 - \omega, \xi\omega, (1 - \xi)\omega, 0)^\top$ such that $\sum_{k=1}^4 \pi_k = 1$. For subsequent sampling occasions, we define transition probability matrices \mathbf{A}_o where each element $\alpha_{k,j}$ is the probability of moving from state k to state j between sampling occasion $o - 1$ and o (and hence $\sum_{j=1}^4 \alpha_{k,j} = 1, \forall k$).

As detailed below, transition matrices for sampling occasions $o > 1$ involve a term for the survival probability of individual i ($\phi_{i,o}$), which is modelled as a function of time between sampling occasions ($\boldsymbol{\delta}$ is a vector of length $O - 1$ storing time differences between sampling occasion dates). We assumed transients are available for detection for a relatively small interval of time before leaving the study area. This process can be represented as a higher apparent mortality rate for transients given the inability to differentiate between emigration and death. We therefore specified survival probability as

$$\phi_{i,o} = \exp(-\kappa_{r_i} \delta_o), \quad r_i \in (1, 0), \quad (2)$$

where r_i is an indicator variable for whether an individual is a resident ($r_i = 1$) or a transient ($r_i = 0$); during prior specification (see below), forcing $\kappa_1 < \kappa_0$ causes resident survival probabilities to be greater than apparent survival probabilities for transients.

For sampling occasions $o > 1$, entry probability (γ_o) for all individuals (see Sections 3.2.1 and 3.2.2 for how τ differentiates entry into resident and transient states) is also modelled as a function of time between sampling occasion, δ_o :

$$\gamma_o = 1 - \exp(-\kappa_\gamma \delta_{o-1}). \quad (3)$$

However, as described in the following two sections, the interpretation and application of each γ_o differs between model parametrizations.

Finally, \mathbf{Y} is a matrix of detection probabilities, where $y_{k,x}$ is the probability of detecting ($x = 2$) or not

detecting ($x = 1$) an individual that is in state k :

$$\mathbf{Y} = \begin{bmatrix} 1 & 0 \\ 1-p & p \\ 1-p & p \\ 1 & 0 \end{bmatrix}. \quad (4)$$

Here p is the detection probability for an individual that has entered the population and is alive, assumed constant across sampling occasions and individuals (residents or transients).

3.2.1 Complete data likelihood

Under the complete data likelihood and data augmentation framework, entry into the marked population can be viewed as a removal process from the superpopulation, whereby an individual from M enters the marked population (Kéry and Schaub, 2012). As such, the number of unentered individuals in M diminishes over the study period. Due to the nature of this removal process, even with assumed constant entry rate, γ_o increases over time on average and lacks biological meaning. The transition probability matrix is thus given by:

$$\mathbf{A}_o = \begin{bmatrix} 1 - \gamma_o & \tau\gamma_o & (1 - \tau)\gamma_o & 0 \\ 0 & \phi_{1,o-1} & 0 & 1 - \phi_{1,o-1} \\ 0 & 0 & \phi_{0,o-1} & 1 - \phi_{0,o-1} \\ 0 & 0 & 0 & 1 \end{bmatrix}, \quad o > 1, \quad (5)$$

where τ is the probability of a newly entered individual being a resident, and $\phi_{1,o-1}$ and $\phi_{0,o-1}$ are survival probabilities for residents and transients.

The transition matrix in Equation 5 defines the latent state process, while Equation 4 is the observation process that is conditional on the latent state process. We initially attempted to model simulated data under the complete data likelihood framework. However, under realistic sample sizes, the very large number of latent states severely strained computer power and memory to the point at which modelling software often crashed during posterior sampling.

3.2.2 Marginalised likelihood

Following methods by Crosbie and Manly (1985), our adaptation of the Schwarz and Arnason model has entry probabilities for each sampling occasion (η_o) conditional on all individuals in N entering during the study period:

$$\eta_o = \begin{cases} b_1, & o = 1 \\ \frac{b_o}{1 - \sum_{u=1}^{o-1} b_u}, & o > 1, \end{cases} \quad (6)$$

where $b_1 = \omega$ is the probability of an individual from N being present during the first sampling occasion. Subsequent b_o entry probabilities are expressed as:

$$b_o = \frac{\gamma_o(1 - b_1)}{\sum_{u=1}^{o-1} \gamma_u}. \quad (7)$$

As such, Equation 6 means $\eta_O = 1$ on the last sampling occasion, and Equation 7 ensures $\sum \mathbf{b} = 1$. Using these conditional η_o entry probabilities, the transition probability matrix is given by:

$$\mathbf{A}_o = \begin{bmatrix} 1 - \eta_o & \tau\eta_o & (1 - \tau)\eta_o & 0 \\ 0 & \phi_{1,o-1} & 0 & 1 - \phi_{1,o-1} \\ 0 & 0 & \phi_{0,o-1} & 1 - \phi_{0,o-1} \\ 0 & 0 & 0 & 1 \end{bmatrix}, \quad o > 1. \quad (8)$$

Just as in the complete data likelihood transition matrix (Equation 5, τ is the probability of a newly entered individual being a resident, and $\phi_{1,o-1}$ and $\phi_{0,o-1}$ are survival probabilities for residents and transients.

Calculating the likelihood contributions of each individual (Equation 1) was done by summing over each individual's latent states via the Forward Algorithm, a dynamic programming algorithm commonly used in hidden Markov modelling (Baum and Petrie, 1966). The Forward Algorithm efficiently calculates the probability of an observed sequence (e.g., an individual's capture history) by summing over the probabilities of all possible latent (latent) state sequences that could result in the observed sequence. Let $\nu_o(k)$ represent the probability an individual is in state k during sampling occasion o given all possible prior latent state sequences. On the first sampling occasion, $\nu_1 = \pi \odot \mathbf{y}(x_1)$, where \odot is the element-wise product. For subsequent occasions ($o > 1$), $\nu_o = \mathbf{A}_o^\top \nu_{o-1} \odot \mathbf{y}(x_o)$. Ultimately, the likelihood contribution of each individual is represented by $\Pr(\mathbf{x}_i | \boldsymbol{\theta}) = \sum \nu_O$. In order to maintain numeric stability and prevent underflow, we calculated log-likelihoods via the Forward Algorithm in log-space while utilizing the log-sum-exp trick (Blanchard et al., 2021).

3.3 Simulations

Data simulations were used to verify that the marginalised likelihood framework could retrieve accurate parameter estimates in Section 3.2.2 and to assess estimation accuracy when constrained by sample size limitations of the goose-beaked whale population. Data were simulated with $\boldsymbol{\delta}$ equivalent to that in the goose-beaked whale dataset, thus simulating data across the study duration with the same spacing and number of sampling occasions. With the exception of N , parameter values were set to the median from posterior distributions of the modelled whale dataset. All parameters were given uniform priors to allow simulated data to drive model convergence. All parameters that were probabilities/proportions and κ_γ had $\text{Unif}(0, 1)$ prior distributions. N was given a uniform prior distribution bounded by the number of detected whales and either 100000 or 10000 depending on the simulation scenario (See below). Mortality rates of residents and transients had non-overlapping uniform prior distributions split by the mean of the simulated mortality rates for the two groups (κ_{mean}), such that residents had $\kappa_1 \sim \text{Unif}(0, \kappa_{mean})$ and transients had $\kappa_0 \sim \text{Unif}(\kappa_{mean}, 1)$. All parameter values, constants, and prior distributions used in simulations are listed in Table 1, and we fit the models via the NIMBLE package in R (R Core Team, 2025; de Valpine et al., 2017, 2024a,b).

In the first simulation scenario, N was set to 10000 to verify that, with a large sample size, the marginalised likelihood framework could retrieve accurate parameter estimates. Given the large sample size and long run time, only one chain was run in this scenario, initialized at the known parameter values and run for 30000 iterations to ensure sufficient effective sample sizes for sampled parameters. In the second simulation scenario, assessing estimation accuracy when constrained by sample size limitations of the goose-beaked whale population, N was set to the posterior median obtained from modelling the whale data

(Table 2). Given the interest in investigating convergence more closely in this second scenario with realistic N , we ran two chains that were initialized as shown in Table 1 and run for 16500 iterations.

Inspection of posterior samples via density and trace plots suggested convergence was likely reached after 3000 samples for both simulation studies, and earlier samples were treated as burn-in and removed from posterior inference. For the second simulation scenario run with two chains, we calculated potential scale reduction factors for each parameter to quantify convergence (Gelman and Rubin, 1992). Additional model diagnostics for both simulation scenarios included autocorrelation and cross-correlation plots, calculation of effective sample sizes, and visual inspection of density and trace plots (Plummer et al., 2006).

Table 1: Simulation inputs and prior distributions for checking that the marginalised likelihood framework can retrieve accurate parameter estimates (“Large population”) and for assessing the degree to which parameters could be accurately estimated when constrained by the limitations of the goose-beaked whale sampling regime (“Realistic population”). With the exception of N in the “Likelihood Check” simulation, values and prior distributions for parameters were set based on posterior medians from the modelled beaked whale data as shown in Section 4.2. The lower bounds for prior distributions on N represent the number of captured individuals, and T is the total study duration across O sampling occasions. Values shown are rounded for clarity.

Parameter	Large population		Realistic population	
	Initial Value	Prior distribution	Initial Values	Prior distribution
N	10000	Unif(1518, 1e5)	5000, 500	Unif(191, 1e4)
ω	0.124	Unif(0, 1)	0.01, 0.1	Unif(0, 1)
ξ	0.377	Unif(0, 1)	0.1, 0.9	Unif(0, 1)
κ_γ	0.081	Unif(0, 1)	1.0, 0.005	Unif(0, 10)
τ	0.080	Unif(0, 1)	0.8, 0.1	Unif(0, 1)
κ_1	1.28e-4	Unif(0, 0.054)	1e-5, 5e-4	Unif(0, 0.001)
κ_0	0.107	Unif(0.054, 1)	0.2, 0.002	Unif(0.001, 1)
p	0.020	Unif(0, 1)	0.01, 0.3	Unif(0, 1)
O	309	—	309	—
T	17.22 years	—	17.22 years	—

3.4 Case study: Goose-beaked whales

Goose-beaked whale capture histories were modelled via the marginalised likelihood framework in Section 3.2.2. Models were fit using the NIMBLE package in R (R Core Team, 2025; de Valpine et al., 2017, 2024a,b). Parameter prior distributions were set similar to those for simulations described above. All parameters that were probabilities/proportions had $\text{Unif}(0, 1)$ prior distributions. Similarly, $\kappa_\gamma \sim \text{Unif}(0, 10)$. N was given a uniform prior distribution bounded by the number of detected whales ($n = 197$) and 10000. Mortality rates of residents and transients had non-overlapping uniform prior distributions; $\kappa_1 \sim \text{Unif}(0, 0.001)$ and $\kappa_0 \sim \text{Unif}(0.001, 1)$.

Two model chains were used, each initialized differently to sample the posterior space. Prior distributions and initial parameter values for each chain are shown in Table 2. Chains were run for 30000 iterations, and inspection of posterior samples via density and trace plots (Plummer et al., 2006) suggested convergence was conservatively reached after 10000 samples, so early samples were removed from posterior summaries as burn-in. Posterior samples were thinned by a factor of 10 (based on observed parameter autocorrelations) solely to increase computational speed when calculating derived quantities by reducing the number of posterior samples used while maintaining relatively large effective sample sizes (Plummer et al., 2006; Link and

Eaton, 2012). We calculated potential scale reduction factors for each parameter to quantify convergence (Gelman and Rubin, 1992). Additional model diagnostics included autocorrelation and cross-correlation plots, calculation of effective sample sizes, and visual inspection of density and trace plots (Plummer et al., 2006).

Abundances of residents and transients at each sampling occasion were derived using N , \mathbf{A}_o (Equation 8), and $\boldsymbol{\pi}$. Posterior distributions of resident and transient abundance during the first sampling occasion were estimated as $N\pi_2$ and $N\pi_3$, respectively. Abundances in subsequent occasions were predicted using \mathbf{A}_o to iteratively transition through sampling occasions and calculate the number of residents (state 2) and transients (state 3) on each occasion.

After obtaining posterior distributions of model parameters, whales captured during the study were classified as resident or transient via the Viterbi Algorithm (Viterbi, 1967). The Viterbi Algorithm used samples from parameters' posterior distributions ($\boldsymbol{\theta}$) to construct \mathbf{A}_o (Equation 8), \mathbf{Y} (Equation 4), and $\boldsymbol{\pi}$, by which it identified the most likely state sequence for each individual over time across parameter posterior samples. Using the $\boldsymbol{\nu}_o$ probabilities of being in a given state on each occasion, the most likely state sequence simply was determined by $\text{argmax}(\boldsymbol{\nu}_o), \forall o$. Ultimately, an individual was classified based on whether more sampled sequences had the individual (entered and alive) as a resident or a transient, and classification confidence scores were calculated as the percentage of samples from $\boldsymbol{\theta}$ that resulted in the predominant classification.

4 Results

4.1 Simulations

Posterior distributions from the first simulation scenario with $N = 10000$ showed that the model parameters are identifiable with sufficient data (Figure 2). Even when constrained by the 17.22-year sampling regime in the goose-beaked whale dataset and low detection probabilities ($p = 0.02$), true parameter values fell within 95% highest posterior density intervals and near the posterior modes. Effective sample sizes were quite small relative to the 27000 posterior iterations remaining after the burn-in period (Figure 2), and this is due to strong autocorrelations within chains for relevant parameters. Two parameters' chains exhibited the best mixing and relatedly had the largest effective samples sizes: detection probability and resident mortality rate (Figure 2). Parameters tightly linked to transient dynamics (e.g., transient apparent mortality rate, abundance) were highly cross-correlated, autocorrelated, and had diffuse posterior distributions despite being centred around the true parameter value.

When further constraining the simulated dataset with $N = 1275$, issues with mixing and parameter identifiability worsened. Under this simulation scenario, transients were never available for capture longer than 11 days (Figure 3), leading to imprecise posterior distributions for γ and ϕ_0 given the sampling regime ($\boldsymbol{\delta}$) and low detection probability. With the exception of τ , the true parameter value fell within 95% highest posterior density intervals (Figure 2). However, posterior distributions were substantially more diffuse and true parameter values were not as consistently located near posterior modes. Model results predicted a 0.963 probability that τ (probability of a newly-entered individual being a resident) was below the true value from the simulation, thus suggesting that the model predicted far too many transients entered the population than truly did in the simulation. Coincidentally, the model predicted 0.934 and 0.882 probabilities of κ_γ and N being greater than the true values, respectively. Despite these poorly estimated parameters, derived

abundance estimates at each sampling occasion showed moderate accuracy, particularly for the latter half of the simulation (Figure 4). However, posterior distribution means for resident abundance were consistently below the true abundance for the first 7 – 8 years of the simulation (Figure 4).

4.2 Case study: Goose-beaked whales

A total of 329 goose-beaked whales were observed during the study period. After filtering the dataset based on the methods described in Section 3.1.1, 197 whales had capture histories retained for modelling. Although 46.7% of modelled capture histories were single sightings (i.e., captured during just one sampling occasion), longer capture histories ranged up to 17.21 years with one whale being captured on 16 different sampling occasions across 11.68 years. Data filtering methods described in Section 3.1.1 removed 229 supplementary sightings, 194 of which were from individuals not included in mark-recapture modelling. Across the 309 sampling occasions, 56.6% had no modelled captures of goose-beaked whales. 66.9% of gaps between sampling occasions were just one day, but 16.9% of gaps were longer than one month (max = 334 days).

Throughout the course of this study, 1306 goose-beaked whales (95% HDPI: 834.4 – 1841.5) were estimated to have entered the San Nicolas Basin (Table 2). Posterior distributions for biological parameters of interest are summarized in Table 2. Abundance estimates for residents and transients across sampling occasions (Figure 5) showed that the San Nicolas Basin contains more resident than transient goose-beaked whales on any given day. With the exception of the initial sampling occasion, during which transient abundance was estimated at its maximum before individuals either emigrated or died, transient abundance appeared constant throughout the study. Meanwhile, resident abundance increased at a near constant rate (Figure 5); resident abundance grew from 59.38 (95% HDPI: 39.12 – 80.11) on 22 October, 2007 to 91.10 (95% HDPI: 68.81 – 113.11) on 5 January, 2025. This equates to a 66.1% growth (95% HDPI: 40.7 – 93.7) over the 17.22-year study. Resident population growth averaged 1.84 (95% HDPI: 0.16 – 3.44) new whales per year.

Table 2: Parameter initialization, prior specification, and resulting estimates for goose-beaked whale modelling. The lower bound for the prior on N represents the total number of whales sighted during days of directed effort across the study period. The modelled whale dataset had 309 sampling occasions (O) spanning 17.22 years (T).

Parameter	Methods		Posterior		
	Initial Values	Prior distribution	Mean (SD)	Median	Mode
N	5000, 500	Unif(197, 1e4)	1305.9 (264.3)	1275.4	1259.6
ω	0.01, 0.1	Unif(0, 1)	0.127 (0.033)	0.124	0.111
ξ	0.1, 0.9	Unif(0, 1)	0.385 (0.104)	0.38	0.384
κ_γ	1.0, 0.005	Unif(0, 10)	0.111 (0.099)	0.08	0.053
τ	0.8, 0.1	Unif(0, 1)	0.084 (0.025)	0.08	0.074
κ_1	1e-5, 5e-4	Unif(0, 0.001)	1.30e-4 (3.18e-5)	1.3e-4	1.33e-4
κ_0	0.2, 0.002	Unif(0.001, 1)	0.121 (0.069)	0.11	0.084
p	0.01, 0.3	Unif(0, 1)	0.019 (1.25e-3)	0.02	0.020

Whales classified (via the Viterbi Algorithm) as transients had capture histories spanning 1-4 days, while resident capture histories spanned 155 days to 17.21 years. Of the 197 sighted whales included in mark-recapture modelling, 107 were classified as transients and 90 as residents. When accounting for supplementary sightings, 22 of the 107 “transients” were captured on more than one sampling occasion, and 10 had

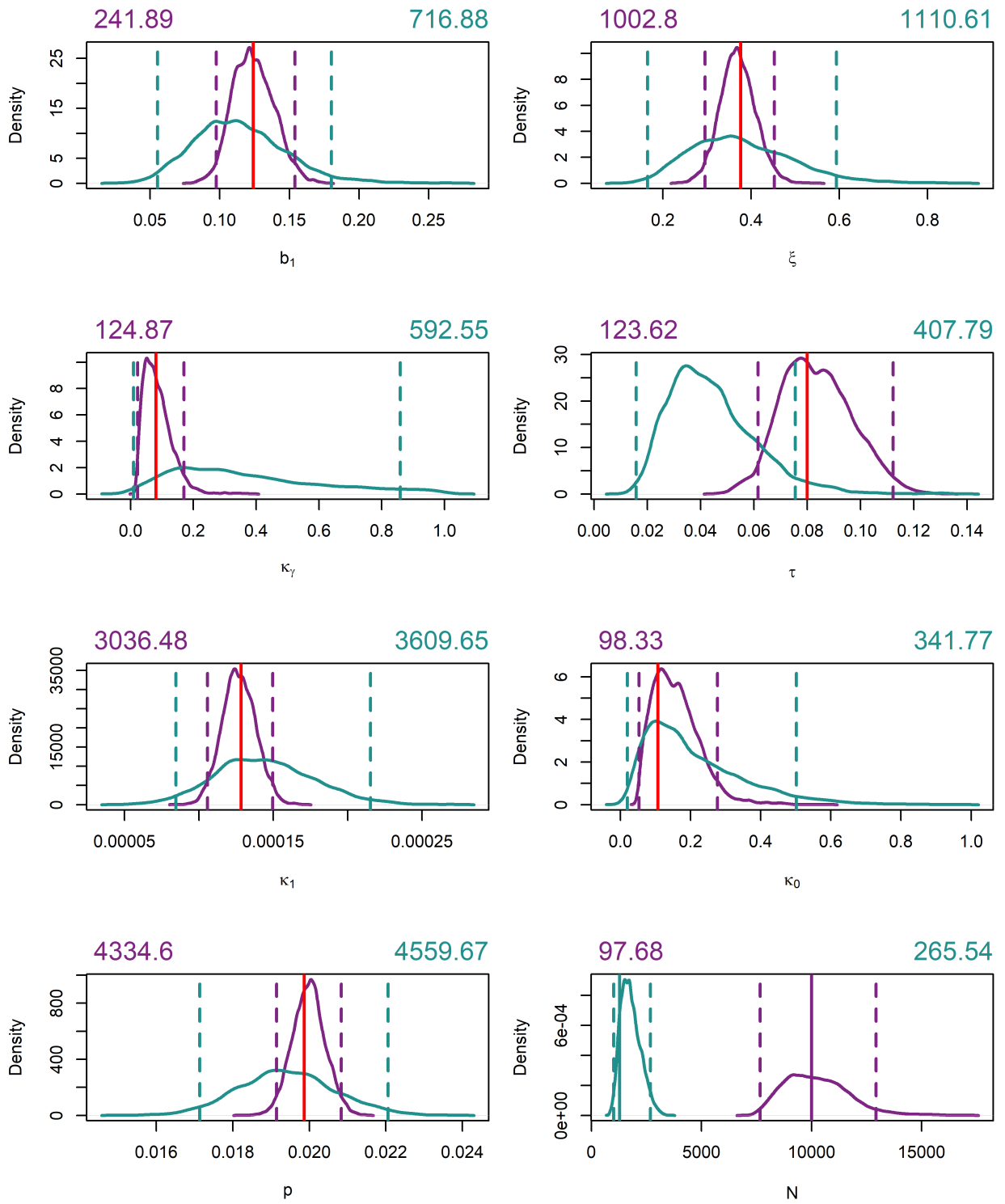


Figure 2: Posterior distributions for parameters of interest from single datasets generated from two simulation scenarios: $N = 10000$ (purple) and $N = 1275$ (green). True parameter values are shown as vertical lines (which are red when both scenarios have the same parameter value); 95% highest posterior density intervals shown by dashed vertical lines. Effective sample sizes are shown above each plot.

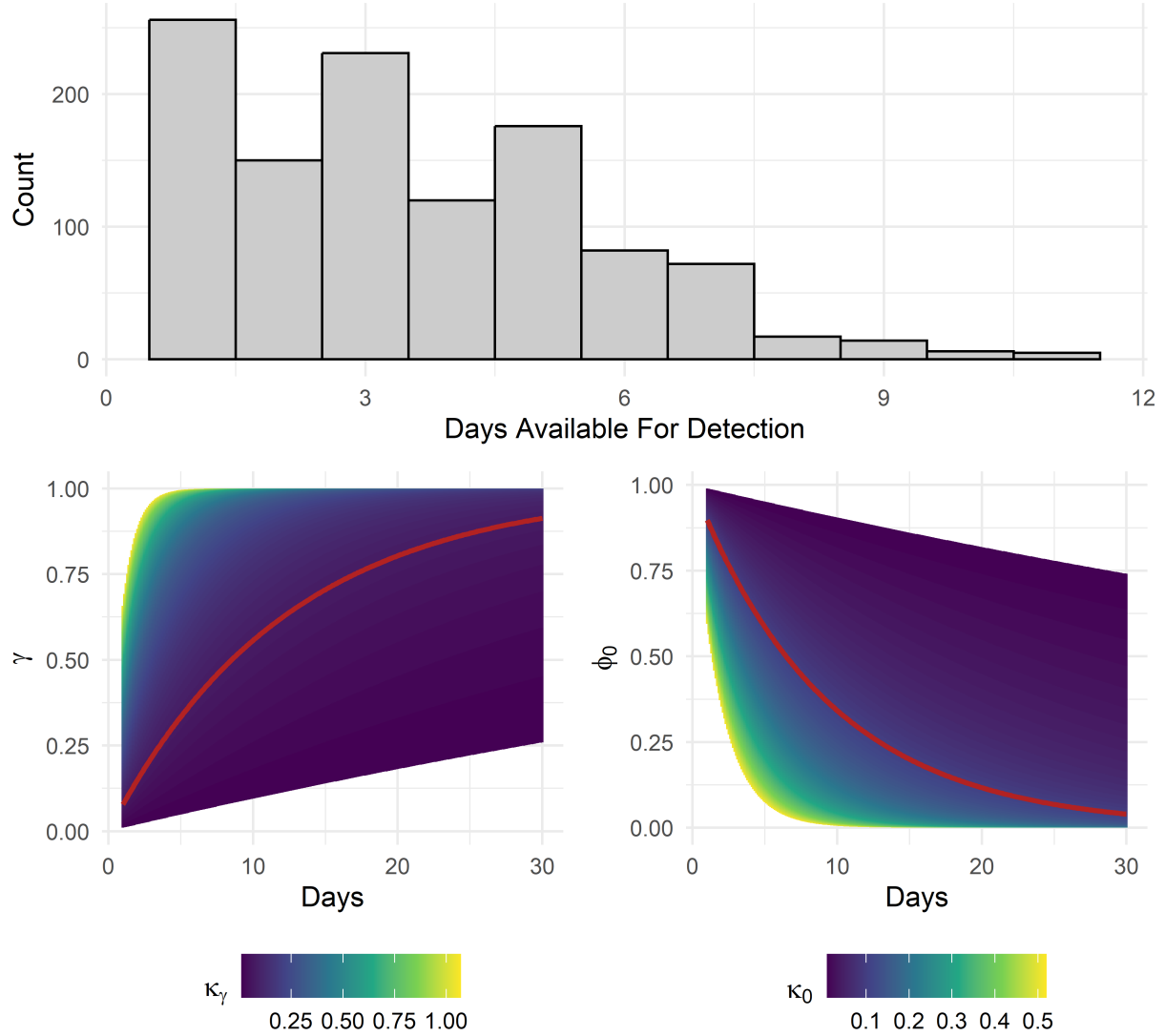


Figure 3: Histogram for the number of days simulated transients were available for capture (top) under the second simulation scenario ($N = 1275$). Bottom plots show derived γ and ϕ_0 probabilities across a range of δ values (spanning about one month) using a range of entry and mortality rates across the posterior distributions from the goose-beaked whale case study (bottom; Table 2). In the bottom plots, medians from each parameter's posterior distribution (i.e., values used in the simulations) are shown in red.

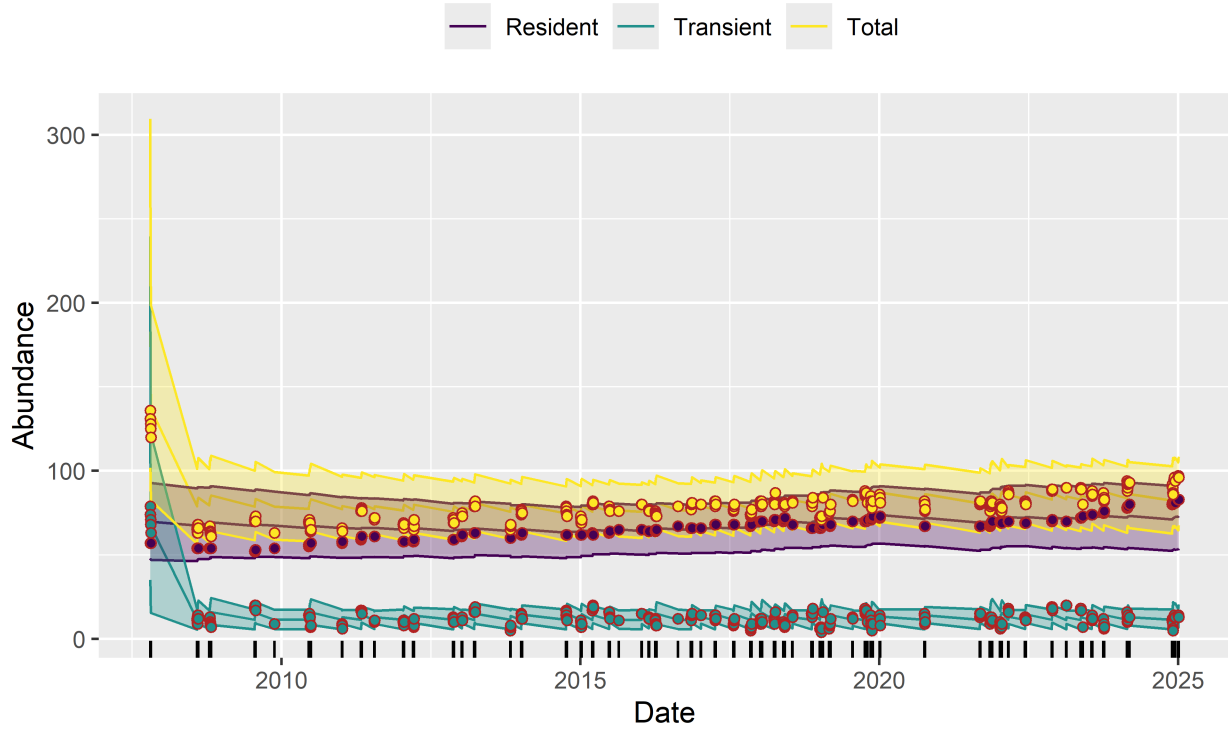


Figure 4: Abundance estimates for simulated individuals based on the mark-recapture model outlined in Section 3.2.2. The simulation was performed using constants and parameter values shown in Table 1 under the “Realistic population” scenario. Total abundance is shown in yellow, while resident and transient abundances are shown in purple and green. True abundances are shown as points that are similarly coloured but have red outlining. Model estimates represent the posterior mean and 95% highest posterior density interval. Sampling occasions are marked by black vertical tick marks along the horizontal axis, although the scale of the horizontal axis makes it impossible to observe all 309 sampling occasions given short gaps between many survey days.

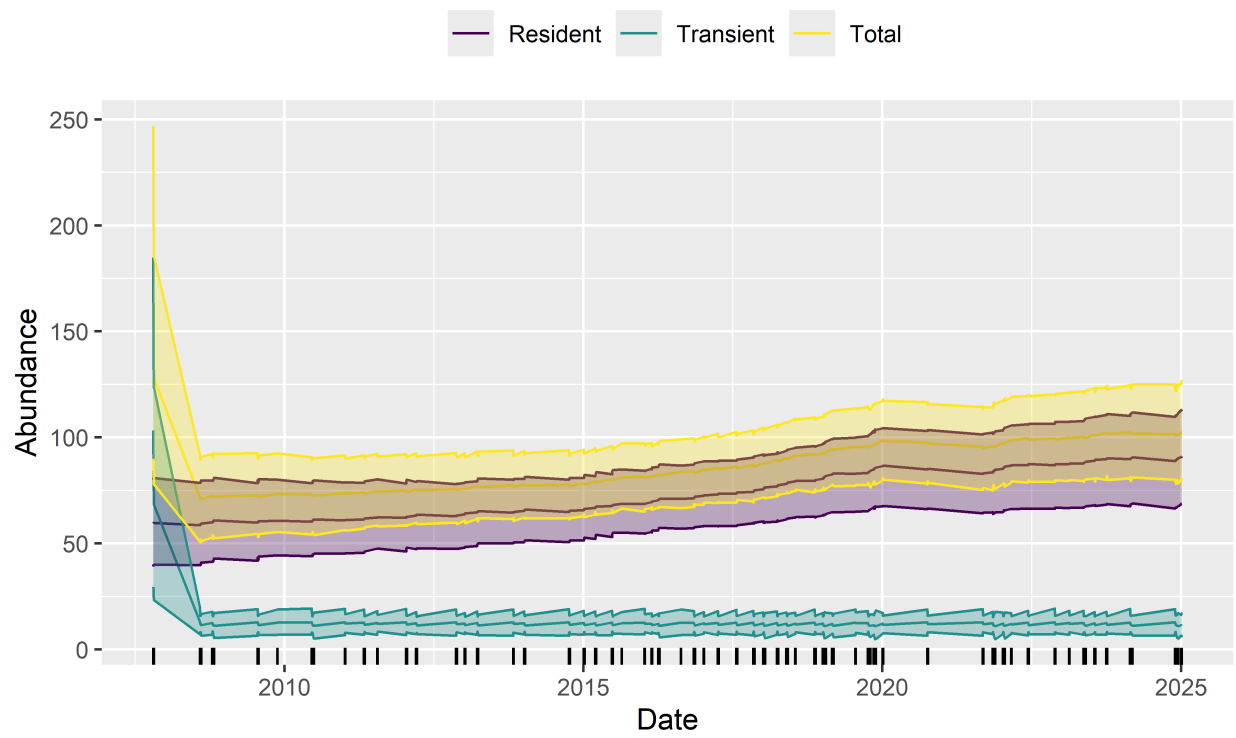


Figure 5: Abundance estimates for goose-beaked whales in Southern California based on the mark-recapture model outlined in Section 3.2.2. Total abundance is shown in yellow, while resident and transient abundances are shown in purple and green. Estimates represent the posterior mean and 95% highest posterior density interval. Sampling occasions are marked by black vertical tick marks along the horizontal axis, although the scale of the horizontal axis makes it impossible to observe all 309 sampling occasions given short gaps between many survey days.

unmodelled (i.e., including supplementary sightings) capture histories spanning more than 4 days. When accounting for supplementary sightings, “transient” whales had capture histories spanning up to 9.92 years. There was one “transient” whale with a capture history spanning 4.77 years that was initially captured (i.e., marked) as a dependent calf. The only sighting for this whale that was retained for modelling was once the whale had aged to become classified as a juvenile (i.e., no longer dependent on the mother).

Of the 55 whales tagged during the study period (Figure 6), the Viterbi Algorithm classified 19 as transients and 30 as residents, while the remaining 6 were not included in the final dataset used for modelling. Confidence scores for Viterbi classifications ranged from 90.1% – 100%, and only three whales (all transients) had classification confidence scores smaller than 99%. While the vast majority of tagged whales remained within the Southern California Bight throughout the duration of respective tag recordings, several whales travelled far distances from deployment locations. Notably, several whales moved south into Mexican waters; two whales classified as residents and one transient approached or swam past Guadalupe Island, Mexico (seen in Figure 6 with latitude/longitude near 29/-118.25). Of these three southwardly travelling whales, the transient was only seen once (no supplementary sightings). The whale classified as a resident that swam south beyond the Baja California Peninsula was captured on three sampling occasions (all used for modelling with two sightings on consecutive days), and these sightings all occurred in January and spanned 10 years (to the exact day). The last of these three whales, also classified as a resident, was only seen on two sampling occasions spanning about 6 months in 2010 – 2011.

5 Discussion

Using ideas and techniques from over half a century of advancements in mark-recapture research, we developed a new open-population mark-recapture model that handles population dynamics in continuous time while accounting for a mixture of residents and transients within the study population. The model was conceptualized with the research objective of differentiating between resident and transient individuals within a population of goose-beaked whales studied in Southern California. Two different model parametrizations were created, one using a complete data likelihood (Section 3.2.1) and one using a marginalised likelihood (Section 3.2.2), which was emphasized in this study given its superior sampling efficiency. Model results from the goose-beaked whale case study (Section 4.2) complement and expand upon previous mark-recapture research for this study population (Curtis et al., 2020). Results from simulations (Section 4.1) showcase both the power of the modelling framework with sufficient data and limitations of the case study results given study constraints.

This study presents the second round of mark-recapture estimates of abundance, survival, and population change for goose-beaked whales in Southern California. Curtis et al. (2020) reported non-calf abundance from a closed-population model to have a posterior distribution mean of 115 ($SD = 49$) for 2015 – 2018 (Huggins, 1989; McClintock, 2015). The largest total abundance (residents and transients) presented in Figure 5 during this same 2015 – 2018 period had a mean of 92.21 (95% HPDI = 74.06 – 109.38). When focusing just on residents during this same time period, we report the largest mean abundance at 79.98 (95% HPDI = 62.52 – 95.87). Curtis et al. (2020) also reported annual survival probability from an open-population Cormack-Jolly-Seber model with a posterior distribution median of 0.954 (Cormack, 1964), and our resident survival probability (when predicted for $\delta = 365$ days) also had a posterior distribution median of 0.954 (Table 2). Curtis et al. (2020) lastly reported an annual rate of change (λ ; Pradel, 1996) with a posterior distribution mean of 0.992 ($SD = 0.029$), thus signifying a likely stable population abundance from

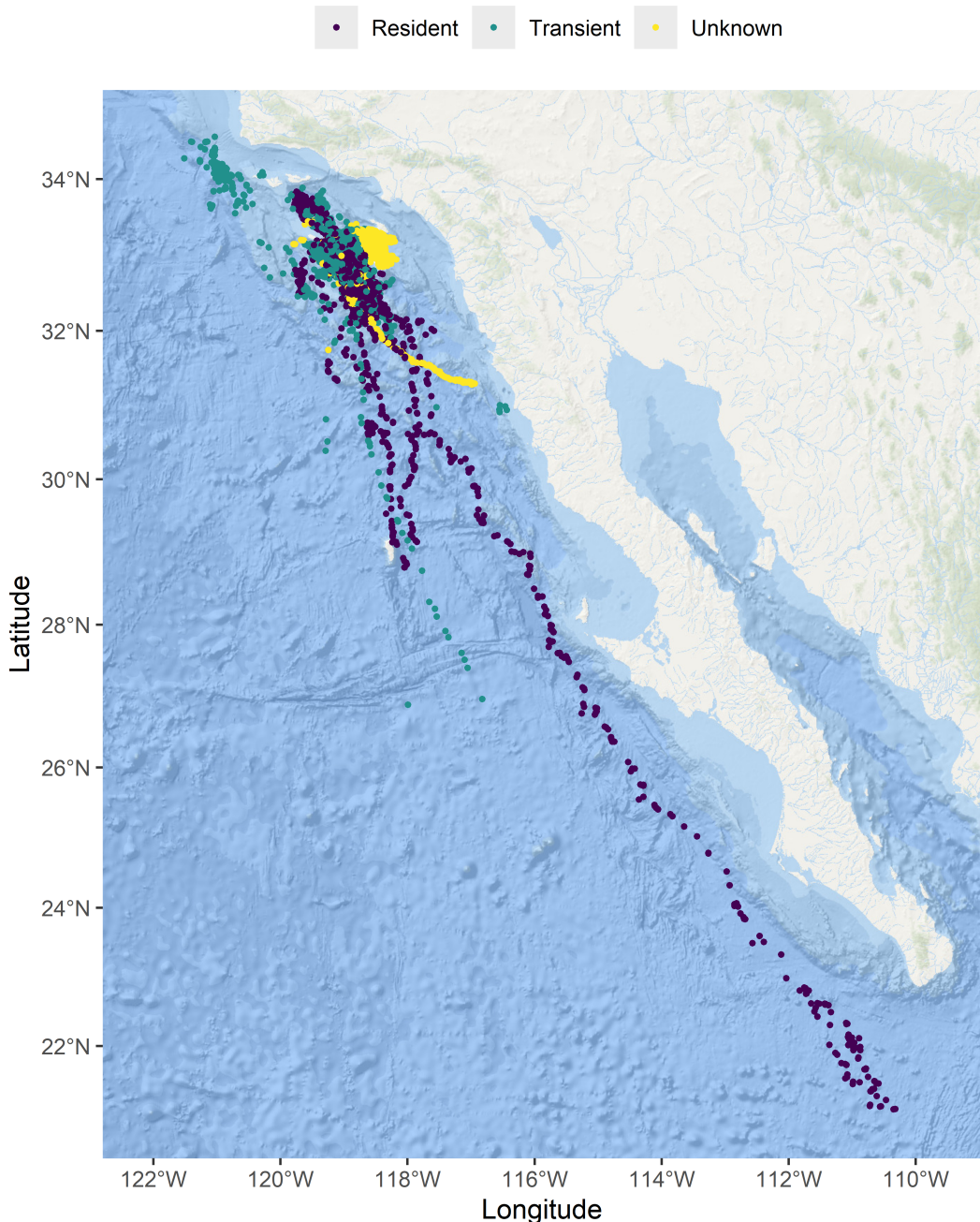


Figure 6: GPS and Argos location estimates for goose-beaked whales tagged in the Southern California Bight. Locations shown were those retained by the Douglas Argos filter. Point colours differentiate between individuals classified as residents or transients based on the Viterbi Algorithm (see Section 3.4). 55 tag deployments are plotted, but many of these are overlapping due to the dense clustering of location estimates around the San Nicolas Basin.

2007 – 2018. Conversely, we report an annual resident population increase of 1.84 (% HDPI: 0.16 – 3.44) new whales per year (see Section 4.2).

While it may be that results presented in this study more accurately depict population dynamics of goose-beaked whales by accounting for transients, it is necessary to caveat these findings given estimation errors presented in our modelled simulations. Low detection probability and complex transient dynamics led to somewhat poor parameter estimation of certain parameters when simulating with a realistic population size (Figure 2). While resident mortality rate (κ_1) was well estimated, entry rate and probabilities of entered individuals being classified as residents lacked precision (wide posterior distributions). This caused poor estimates of resident abundance during the first sampling occasion and led to overestimated resident abundance for 7 – 8 years until underestimated resident entry rate (due to overestimated κ_γ and underestimated τ) resulted in resident abundance estimates close to the true simulated values (Figure 4). Given these simulation results, it may be that our model of goose-beaked whale data contains overestimated resident abundances for early years in the study, which would mean population growth rate was also underestimated in this study. However, it must be mentioned that this study (and that of Curtis et al., 2020) did not perform any goodness-of-fit tests (e.g., χ^2 test, which is popular in mark-recapture models) to measure how well the model fit the observed data. Poor fit to the observed data would make any inferences made from the model invalid. Continued mark-recapture modelling efforts for this population must utilize such goodness-of-fit tests or else risk improper population management decisions being made based on misleading model results.

Transient dynamics are inherently difficult to estimate with precision. When transients are only available for capture during a short window of time (i.e., low apparent survival), low detection probability and large gaps between sampling occasions (as observed in this study) cause many transient individuals to enter and leave the study area completely undetected. For individuals that are detected, estimates on rates of entry and apparent mortality are very uncertain without observing the first and last sampling occasions during which individuals were present across a sufficient number of unique individuals. Simulations where $\boldsymbol{\theta}$ was set to the posterior medians from the modelled beaked whale data (Table 2) showed that transients are not available for capture more than 11 days. Coupled with low detection probability and constraints of the sampling regime ($\boldsymbol{\delta}$), this resulted in very uncertain estimates for γ and ϕ_0 (Figure 3). Figure 3 also indicates that scaled entry probabilities (\mathbf{b}) are essentially equivalent for larger posterior samples of κ_γ and longer δ_o , which leads to large uncertainty in the number of transients that entered and left the study site (and thus large uncertainty in N) during long gaps between sampling occasions.

We assumed a constant detection probability across individuals and sampling occasions. However, one of the benefits of our custom Bayesian model implementation is the ease with which we can account for likely heterogeneity in detection probabilities. The mark-recapture model in Curtis et al. (2020) modelled individual- and occasion-specific detection probabilities via a logit-linear function that incorporated both a random effect to account for individual heterogeneity and the effect of survey effort in low Beaufort sea states. They found that increased vessel effort significantly increased detection probability, which encourages us to explore a similar approach going forward. A recently published method for modelling heterogeneity in detection probability within a Jolly-Seber model incorporates telemetry and survey effort data to account for spatio-temporal sampling bias (Badger et al., 2024), and we could compare model fit using these methods with those just described from (Curtis et al., 2020) via WAIC or similar relative measures for goodness-of-fit. Curtis et al. (2020) also incorporated the methods of McClintock et al. (2013), which allowed for modelling of bilateral captures histories via the multimark package in R (McClintock, 2015), thus increasing their sample size and accounting for uncertainty about the number of distinct animals captured. We did not replicate

these methods (instead only used one-sided captures of whales), but doing so in the future could increase detection probability and improve model precision.

Prior to model development, we considered the use of spatial mark-recapture methods to better account for unmodelled individual heterogeneity in capture probabilities. By recognizing that individuals' capture probabilities are spatially dependent, a detection function can be used to model detection probability as a function of distance between the location where an individual was captured ("traps") and their latent "activity centre" (Royle et al., 2013). Thus, what appears as individual heterogeneity in non-spatial mark-recapture may be explained by individuals' space use (i.e., home range and movement patterns). Spatial capture-recapture models have been constructed for marine mammal surveys, where a spatial grid has defined trap locations, and individuals are detected in grid cells as vessels move along regular transect lines while entering and exiting gridded "traps" (Pirotta et al., 2015; Glennie et al., 2021). We did not employ these methods primarily because the nature of direct survey effort around SOAR is non-standard given the behaviour of goose-beaked whales and how we coordinated search effort to maximize captures based on acoustic detections made with the M3R system (Jarvis et al., 2014). During surveys with directed effort in the San Nicolas Basin, the probability of detecting an individual at a specific location changed given various situations that are difficult to quantify and incorporate into a detection function. For example, if directed by M3R acousticians towards distant vocal detections, survey teams often transited at high speeds to get near the acoustic detection location, at which point the vessel was sometimes set to drift while the field team scanned and listened for surfacing whales. At other times, the field team might have slowly transited around an area suspected of having whales or known to historically be an area of high density (if no acoustic detections were made recently). Other scenarios also existed. Therefore, how surveys were conducted depended heavily on recent acoustic activity, weather, the location of the survey vessel, how many people were onboard the vessel, the time of day, and many other constantly changing factors. While future expansion in spatial mark-recapture methods could be developed to account for regularly changing effort strategies, such work was beyond the time and scope of this project.

Related to the issue of heterogeneity in detection probability is the issue of temporary emigration and subsequent re-immigration. Seasonal and oceanographic factors have been shown to significantly predict changes in goose-beaked whale acoustic densities within the San Nicolas Basin (Moretti et al., 2018; Schoenbeck et al., 2024). Goose-beaked whales were also observed avoiding SOAR during and following sonar exposures (Jones-Todd et al., 2022). It may be speculated that goose-beaked whales conduct occasional "maintenance migrations", like Antarctic killer whales (*Orcinus orca*), to warmer waters given accumulations of diatoms on some whales (Durban and Pitman, 2012; Coomber et al., 2022). Temporary emigration and re-immigration are also clearly shown in Figure 6, perhaps most extremely with the whale classified as a resident that travelled beyond the southern tip of the Baja California Peninsula and was then recaptured 10 years later. In the present study, concerns regarding identifiability between detection probability and availability for detection led to the exclusion of emigration and re-immigration parameters. Future modelling attempts may account for seasonal changes in relative abundance (perhaps using concurrent acoustic densities or summaries of relative density change over time), avoidance responses caused by sonar, and unexposed baseline movements to improve occasion-specific detection probabilities.

Temporary emigration and re-immigration may also be caused by complex metapopulation dynamics not accounted for in this model. Put more plainly, goose-beaked whale residency in Southern California may be more appropriately characterized along a spectrum rather than two discrete groups. Given the presence of a distinct resident population of goose-beaked whales nearby at Guadalupe Island, México (Cárdenas-Hinojosa

et al., 2015), to which two of our tagged whales travelled, and detections of goose-beaked whales along the entire western coast of the United States (Moore and Barlow, 2013; Barlow et al., 2022), it is possible that the Southern California Bight functions in multiple ways: a home for hyper-resident goose-beaked whales, a stop-over site for frequently visiting goose-beaked whales, a good place to travel through (to forage, mate, etc.) for life-long transients, etc. Similar such dynamics have been presented based on tag and photo-identification evidence from fin whales (*Balaenoptera physalus*) cohabiting Southern California (Lagerquist et al., 2024; Falcone et al., 2022).

In the context of a multi-state model, handling of temporary emigration and subsequent re-immigration is best done by increasing the number of states (e.g., separate states for alive/present and alive/absent). Increasing the number of states can also allow estimation of age- and sex-specific vital rates, as has been done previously for a population of goose-beaked whales in the Ligurian Sea (Tenan et al., 2023). While accounting for transients, separate classes based on whales' life histories (e.g., calves, male or female juveniles, reproductive female, mature male, etc.) could reveal trends in the age/sex classes that transients exhibit when captured and could separate population entry into immigration and birth processes. However, lower recapture rates in Southern California compared to the Ligurian Sea may hinder precise estimation of these additional parameters in θ (Curtis et al., 2020; Tenan et al., 2023).

In addition to the possibility that the elevated initial abundance of transients (Figure 5) was simply due to data limitations and the first sampling occasion being handled differently than subsequent occasions given $\delta_{o=1}$ is undefined, it is also possible that this result hints at non-constant entry and apparent mortality rates. To account for variation in entry and mortality rates, we would instead have to define κ_γ and κ_{r_i} for $r \in (0, 1)$ as “hazard” functions spanning the duration of the study that describe variation in the dynamic processes over time (Rushing, 2023; Fouchet et al., 2016; Murray and Sandercock, 2019; Choquet et al., 2017). Just taking survival probability as an example in detailing the approach, Equation 2 would become:

$$\phi_{i,o} = \exp\left(-\int_o^{o+1} \kappa_{r_i}(u)du\right), \quad r_i \in (1, 0), \quad (9)$$

where $\kappa_{r_i}(u)$ is the hazard function being integrated over the time between sampling occasions. Considering goose-beaked whales in Southern California, entry and mortality hazard functions could be defined by changes in oceanographic conditions, anthropogenic activity, or density-dependence (Oro and Doak, 2020; Schoenbeck et al., 2024; Williams et al., 2013; Wiggins et al., 2018; Moretti et al., 2018).

If our model results have correctly identified a growing resident population (given model improvements, bias, and unknown goodness-of-fit as discussed above), it must next be determined whether this indicates a healthy, growing resident population or whether Southern California is an “ecological trap” or “population sink” (Battin, 2004; Forney et al., 2017). As also discussed by Curtis et al. (2020), resident animals may have reduced fitness due to cumulative, sublethal effects of foraging disruption as caused by frequent exposure to sonar and other anthropogenic noise (Hin et al., 2023). If this is the case, residents may be dying off while simultaneously being replaced at a higher rate by transients from the metapopulation. It may be, however, that a growing resident population is indeed due to entry rate being higher than the mortality rate. Expanding our multi-state model to include age/sex classes and separate entry into birth and immigration processes could help differentiate between these explanations for resident population growth.

Incorporating the differentiation between resident and transient individuals into a population consequences of disturbance (PCoD) model could also help uncover complex underlying population dynamics. Incorporating classifications of captured whales based on the Viterbi Algorithm (or some other metric de-

scribing residency) could help explain variation in sonar responses exhibited by goose-beaked whales around SOAR (DeRuiter et al., 2013; Falcone et al., 2017; Jones-Todd et al., 2022). Differential residency could also inform models of long-term aggregate sonar exposure levels, where transients could be exposed less frequently (but perhaps respond more strongly due to lack of habituation) to sonar (Joy et al., 2022). These interconnected components could ultimately be incorporated into PCoD models that, for the first time, predict effects of sonar exposure on population dynamics given different affects on resident and transient individuals' health and vital rates (Hin et al., 2023; Pirotta et al., 2022b).

This study presents the first attempt to differentiate between resident and transient goose-beaked whales using a newly developed open-population mark-recapture model. While these results are preliminary, given aforementioned biases and suggestions for model improvements, and should not be used explicitly for population management decisions, they provide a foundation for future analyses. Future modelling efforts should initially aim to improve estimates of detection probabilities, which will in turn enhance model accuracy for other biological metrics. Simulations should then be used to determine the feasibility of expanding the model to incorporate additional states (e.g., age/sex classes or more than two levels of residency), non-constant entry and mortality rates (e.g., Equation 9), and temporary emigration and re-immigration. Lastly, and perhaps most importantly, goodness-of-fit tests should be employed to validate statistical inferences. The custom model code made available as part of this project should foster rapid and easy implementation of these suggested model improvements. We hope this study acts as a launching pad for future research to inform and enhance population monitoring and conservation efforts for goose-beaked whales in Southern California.

6 Acknowledgements

Thanks to all project members, collaborators, funders, and supporters for their continual aid in this research, especially Len Thomas, Enrico Pirotta, Greg Schorr, and Erin Falcone for their research supervision and flexibility to allow me to complete my dissertation remotely while living with my wife back in the USA. A huge thanks also to my amazing wife, Stephanie Sweeney, for her unconditional love and for the countless personal sacrifices she makes for my work. Thank you also to my parents (Doug and Wilma Sweeney) and in-laws (Dave and Joanie Praamsma), for the support this past year while I was studying abroad. My gratitude also goes out to everyone in my wonderful community in St Andrews (CREEM colleagues, fellow students, Cornerstone church, and my neighbours) that filled my life with extra joy beyond the office.

6.1 Funding

This material is based in part upon work supported by the Naval Facilities Engineering and Expeditionary Warfare Center under contract No. N39430-16-C-1870 and N39430-170C-1985, and in part by funding received from the US Navy's Pacific Fleet under contract No's. N66604-14-Q-0145, N66604-18-P-2187, N62473-19-2-0025, and N66604-22-D-F200.

6.2 Data ethics and availability

Model code and data to fit the model are stored in a GitHub repository ([ZcTransCMR](#)), available upon request. Data collection for this study was principally conducted by MarEcoTel and their project collaborators. All field work occurred under US National Marine Fisheries Service permits and was approved by

Institutional Animal Care and Use (IACUC) protocols. More information on permit numbers and IACUC reviews can be provided upon request. This study was completed as part of a larger research project approved by the University of St Andrews' School of Biology Ethics Committee (BL18267 and BL18253).

6.3 Declaration statement

I, David Sweeney (signature below), declare that this thesis is my own work completed under the supervision and guidance of Prof. Len Thomas and Dr. Enrico Pirotta. This work was completed while enrolled in the MSc Statistics program at the University of St Andrews for the 2024/25 academic year. This research has not been previously submitted elsewhere.

The image shows two handwritten signatures side-by-side. The signature on the left appears to be 'David Sweeney' and the signature on the right appears to be 'Len Thomas'.

7 References

- Adams, J., Jump, W. A., Burton, E. J., and Harvey, J. T. (2015). Stomach contents of a Cuvier's beaked whale (*Ziphius cavirostris*) stranded in Monterey Bay, California. *Northwestern Naturalist*, 96(1):93–98.
- Aguilar Soto, N., Johnson, M., Madsen, P. T., Tyack, P. L., Bocconcelli, A., and Fabrizio Borsani, J. (2006). Does intense ship noise disrupt foraging in deep-diving cuvier's beaked whales (*Ziphius cavirostris*)? *Marine Mammal Sci*, 22(3):690–699.
- Andrews, R. D., Baird, R. W., Calambokidis, J., Goertz, C. E. C., Gulland, F. M. D., Heide-Jørgensen, M. P., Hooker, S. K., Johnson, M., Mate, B., Mitani, Y., Nowacek, D. P., Owen, K., Quakenbush, L. T., Raverty, S., Robbins, J., Schorr, G. S., Shpak, O. V., Townsend, F. I., Uhrt, M., Wells, R. S., and Zerbini, A. N. (2019). Best practice guidelines for cetacean tagging. *J. Cetacean Res. Manage.*, 20:27–66.
- Auster, P. and Watling, L. (2009). Beaked whale foraging areas inferred by gouges in the seafloor. *Marine Mammal Science*, 26(1):226–233.
- Badger, J. J., Johnson, D. S., Baird, R. W., Bradford, A. L., Kratofil, M. A., Mahaffy, S. D., and Oleson, E. M. (2024). Incorporating telemetry information into capture-recapture analyses improves precision and accuracy of abundance estimates given spatiotemporally biased recapture effort. *Methods in Ecology and Evolution*, 15(10):1847–1858.
- Baird, R. W., Webster, D. L., McSweeney, D. J., Ligon, A. D., Schorr, G. S., and Barlow, J. (2006). Diving behaviour of Cuvier's (*Ziphius cavirostris*) and Blainville's (*Mesoplodon densirostris*) beaked whales in Hawai'i. *Can. J. Zool.*, 84(8):1120–1128.
- Barlow, J. (2015). Inferring trackline detection probabilities, $g(0)$, for cetaceans from apparent densities in different survey conditions. *Mar Mam Sci*, 31(3):923–943.
- Barlow, J., Ferguson, M. C., Perrin, W. F., Ballance, L., Gerrodette, T., Joyce, G., Mullin, K., Palka, D. L., and Waring, G. (2006). Abundance and densities of beaked and bottlenose whales (family Ziphiidae).

- Barlow, J., Moore, J. E., McCullough, J. L. K., and Griffiths, E. T. (2022). Acoustic-based estimates of Cuvier's beaked whale (*Ziphius cavirostris*) density and abundance along the U.S. West Coast from drifting hydrophone recorders. *Marine Mammal Science*, 38(2):517–538.
- Barlow, J., Schorr, G. S., Falcone, E. A., and Moretti, D. J. (2020). Variation in dive behavior of Cuvier's beaked whales with seafloor depth, time-of-day, and lunar illumination. *Mar. Ecol. Prog. Ser.*, 644:199–214.
- Battin, J. (2004). When Good Animals Love Bad Habitats: Ecological Traps and the Conservation of Animal Populations. *Conservation Biology*, 18(6):1482–1491.
- Baum, L. E. and Petrie, T. (1966). Statistical Inference for Probabilistic Functions of Finite State Markov Chains. *The Annals of Mathematical Statistics*, 37(6):1554–1563.
- Baumann-Pickering, S., Roch, M. A., Brownell Jr, R. L., Simonis, A. E., McDonald, M. A., Solsona-Berga, A., Oleson, E. M., Wiggins, S. M., and Hildebrand, J. A. (2014). Spatio-temporal patterns of beaked whale echolocation signals in the North Pacific. *PLoS ONE*, 9(1):e86072.
- Belda, E. J., Barba, E., and Monrós, J. S. (2007). Resident and transient dynamics, site fidelity and survival in wintering Blackcaps *Sylvia atricapilla*: Evidence from capture–recapture analyses. *Ibis*, 149(2):396–404.
- Bernaldo De Quirós, Y., Fernandez, A., Baird, R. W., Brownell, R. L., Aguilar De Soto, N., Allen, D., Arbelo, M., Arregui, M., Costidis, A., Fahlman, A., Frantzis, A., Gulland, F. M., Iñíguez, M., Johnson, M., Komnenou, A., Koopman, H., Pabst, D. A., Roe, W. D., Sierra, E., Tejedor, M., and Schorr, G. (2019). Advances in research on the impacts of anti-submarine sonar on beaked whales. *Proceedings of the Royal Society B: Biological Sciences*, 286(1895).
- Blanchard, P., Higham, D. J., and Higham, N. J. (2021). Accurately computing the log-sum-exp and softmax functions. *IMA J Numer Anal*, 41(4):2311–2330.
- Boldrocchi, G., Conte, L., Galli, P., Bettinetti, R., and Valsecchi, E. (2024). Cuvier's beaked whale (*Ziphius cavirostris*) detection through surface-sourced eDNA: A promising approach for monitoring deep-diving cetaceans. *Ecological Indicators*, 161:111966.
- Cárdenas-Hinojosa, G., Hoyos-Padilla, M., and Rojas-Bracho, L. (2015). Occurrence of Cuvier's beaked whales (*Ziphius cavirostris*) at Guadalupe Island, Mexico, from 2006 to 2009. *Latin American Journal of Aquatic Mammals*, 10(1):38.
- Cholewiak, D., DeAngelis, A. I., Palka, D., Corkeron, P. J., and Van Parijs, S. M. (2017). Beaked whales demonstrate a marked acoustic response to the use of shipboard echosounders. *R. Soc. open sci.*, 4(12):170940.
- Choquet, R., Garnier, A., Awuve, E., and Besnard, A. (2017). Transient state estimation using continuous-time processes applied to opportunistic capture–recapture data. *Ecological Modelling*, 361:157–163.
- Coates, S. N., Sweeney, D. A., Falcone, E. A., Watwood, S. L., Rone, B. K., DeRuiter, S. L., Barlow, J., Dolan, K. A., Morrissey, R. P., DiMarzio, N. A., Jarvis, S. M., Andrews, R. D., and Schorr, G. S. (2024). Insights into foraging behavior from multi-day sound recording tags on goose-beaked whales (*Ziphius cavirostris*) in the Southern California Bight. *Front. Mar. Sci.*, 11:1415602.

- Conn, P. B., Gorgone, A. M., Jugovich, A. R., Byrd, B. L., and Hansen, L. J. (2011). Accounting for transients when estimating abundance of bottlenose dolphins in Choctawhatchee Bay, Florida. *The Journal of Wildlife Management*, 75(3):569–579.
- Coomber, F. G., Falcone, E. A., Keene, E. L., Cárdenas-Hinojosa, G., Huerta-Patiño, R., and Rosso, M. (2022). Multi-regional comparison of scarring and pigmentation patterns in Cuvier's beaked whales. *Mamm Biol.*
- Cormack, R. M. (1964). Estimates of Survival from the Sighting of Marked Animals. *Biometrika*, 51(3/4):429–438.
- Cox, T. M., Ragen, T. J., Read, A. J., Vos, E., Baird, R. W., Balcomb, K., Barlow, J., Caldwell, J., Cranford, T., Crum, L., D'Amico, A., D'spain, G., Fernández, A., Finneran, J., Gentry, R., Gerth, W., Gulland, F., Hildebrand, J., Housser, D., Hullar, T., Jepson, P. D., Ketten, D., Macleod, C. D., Miller, P., Moore, S., Mountain, D. C., Palka, D., Ponganis, P., Rommel, S., Rowles, T., Taylor, B., Tyack, P., Wartzok, D., Gisiner, R., Meads, J., and Benner, L. (2006). Understanding the impacts of anthropogenic sound on beaked whales. *Journal of cetacean research and management*, 7(3):177–187.
- Crosbie, S. F. and Manly, B. F. J. (1985). Parsimonious Modelling of Capture-Mark-Recapture Studies. *Biometrics*, 41(2):385–398.
- Curtis, K. A., Moore, J. E., Falcone, E. A., Moretti, D. J., Schorr, G. S., Barlow, J., and Keene, E. (2020). Abundance, survival, and annual rate of change of Cuvier's beaked whales (*Ziphius cavirostris*) on a Navy sonar range. *Marine Mammal Science*, pages 1–21.
- Czapanskiy, M. F., Savoca, M. S., Gough, W. T., Segre, P. S., Wisniewska, D. M., Cade, D. E., and Goldbogen, J. A. (2021). Modelling short-term energetic costs of sonar disturbance to cetaceans using high-resolution foraging data. *Journal of Applied Ecology*, 58(8):1643–1657.
- de Valpine, P., Paciorek, C., Turek, D., Michaud, N., Anderson-Bergman, C., Obermeyer, F., Wehrhahn Cortes, C., Rodríguez, A., Temple Lang, D., and Paganin, S. (2024a). NIMBLE: MCMC, particle filtering, and programmable hierarchical modeling.
- de Valpine, P., Paciorek, C., Turek, D., Michaud, N., Anderson-Bergman, C., Obermeyer, F., Wehrhahn Cortes, C., Rodríguez, A., Temple Lang, D., and Paganin, S. (2024b). *NIMBLE User Manual*.
- de Valpine, P., Turek, D., Paciorek, C., Anderson-Bergman, C., Temple Lang, D., and Bodik, R. (2017). Programming with models: Writing statistical algorithms for general model structures with NIMBLE. *Journal of Computational and Graphical Statistics*, 26(2):403–413.
- DeRuiter, S. L., Southall, B. L., Calambokidis, J., Zimmer, W. M., Sadykova, D., Falcone, E. A., Friedlander, A. S., Joseph, J. E., Moretti, D., Schorr, G. S., Thomas, L., and Tyack, P. L. (2013). First direct measurements of behavioural responses by Cuvier's beaked whales to mid-frequency active sonar. *Biology Letters*, 9(4):1–5.
- Douglas, D. C., Weinzierl, R., C Davidson, S., Kays, R., Wikelski, M., and Bohrer, G. (2012). Moderating Argos location errors in animal tracking data. *Methods in Ecology and Evolution*, 3(6):999–1007.
- Dujon, A. M., Lindstrom, R. T., and Hays, G. C. (2014). The accuracy of Fastloc-GPS locations and implications for animal tracking. *Methods in Ecology and Evolution*.

- Durban, J. W. and Pitman, R. L. (2012). Antarctic killer whales make rapid, round-trip movements to subtropical waters: Evidence for physiological maintenance migrations? *Biology Letters*, 8(2):274–277.
- Faerber, M. M. and Baird, R. W. (2010). Does a lack of observed beaked whale strandings in military exercise areas mean no impacts have occurred? A comparison of stranding and detection probabilities in the Canary and main Hawaiian Islands. *Marine Mammal Science*.
- Fahlman, A. (2023). Cardiorespiratory adaptations in small cetaceans and marine mammals. *Experimental Physiology*.
- Fahlman, A., Moore, M. J., and Wells, R. S. (2021). How do marine mammals manage and usually avoid gas emboli formation and gas embolic pathology? Critical clues from studies of wild dolphins. *Front. Mar. Sci.*, 8:598633.
- Fahlman, A., Tyack, P. L., Miller, P. J. O., and Kvadsheim, P. H. (2014). How man-made interference might cause gas bubble emboli in deep diving whales. *Frontiers in Physiology*, 5.
- Falcone, E., Schorr, G., Keene, E., Massimiliano Rosso, Frazer Coomber, Simone Tenan, Andrew Read, Danielle Waples, Will Cioffi, Gustavo Cárdenas Hinojosa, Rodrigo Huerta Patiño, Fleur Visser, and Machiel Oudejans (2025). Vital Rates of Cuvier's beaked whales: A multi-regional comparative assessment. ONR Final Report N000142112563, MarEcoTel.
- Falcone, E. A., Keene, E. L., Keen, E. M., Barlow, J., Stewart, J., Cheeseman, T., Hayslip, C., and Palacios, D. M. (2022). Movements and residency of fin whales (*Balaenoptera physalus*) in the California Current System. *Mamm Biol*.
- Falcone, E. A., Schorr, G. S., Watwood, S. L., DeRuiter, S. L., Zerbini, A. N., Andrews, R. D., Morrissey, R. P., and Moretti, D. J. (2017). Diving behaviour of Cuvier's beaked whales exposed to two types of military sonar. *Royal Society Open Science*, 4(8):170629.
- Fearnbach, H., Durban, J., Parsons, K., and Claridge, D. (2012). Photographic mark–recapture analysis of local dynamics within an open population of dolphins. *Ecological Applications*, 22(5):1689–1700.
- Feyrer, L. J., Stanistreet, J. E., and Moors-Murphy, H. B. (2024). Navigating the unknown: Assessing anthropogenic threats to beaked whales, family Ziphiidae. *R. Soc. Open Sci.*, 11(4):240058.
- Fiedler, P. C., Becker, E. A., Forney, K. A., Barlow, J., and Moore, J. E. (2023). Species distribution modeling of deep-diving cetaceans. *Marine Mammal Science*, 39(4):1178–1203.
- Filadelfo, R., Pinelis, Y. K., Davis, S., Chase, R., Mintz, J., Wolfanger, J., Tyack, P. L., Ketten, D. R., and D'Amico, A. (2009). Correlating whale strandings with Navy exercises off southern California. *aquatic mammals*, 35(4):445–451.
- Forney, K., Southall, B., Slooten, E., Dawson, S., Read, A., Baird, R., and Brownell, R. (2017). Nowhere to go: Noise impact assessments for marine mammal populations with high site fidelity. *Endangered Species Research*, 32:391–413.
- Fouchet, D., Santin-Janin, H., Sauvage, F., Yoccoz, N. G., and Pontier, D. (2016). An r package for analysing survival using continuous-time open capture–recapture models. *Methods in Ecology and Evolution*, 7(5):518–528.

- Fregosi, S., Harris, D. V., Matsumoto, H., Mellinger, D. K., Barlow, J., Baumann-Pickering, S., and Klinck, H. (2020). Detections of whale vocalizations by simultaneously deployed bottom-moored and deep-water mobile autonomous hydrophones. *Front. Mar. Sci.*, 7:721.
- Gelman, A. and Rubin, D. B. (1992). Inference from Iterative Simulation Using Multiple Sequences. *Statistical Science*, 7(4):457–472.
- Genovart, M. and Pradel, R. (2019). Transience effect in capture-recapture studies: The importance of its biological meaning. *PLOS ONE*, 14(9):e0222241.
- Gimenez, O., Rossi, V., Choquet, R., Dehais, C., Doris, B., Varella, H., Vila, J.-P., and Pradel, R. (2007). State-space modelling of data on marked individuals. *Ecological Modelling*, 206(3):431–438.
- Glennie, R., Thomas, L., Speakman, T., Garrison, L., Takeshita, R., and Schwacke, L. (2021). Estimating spatially-varying density and time-varying demographics with open population spatial capture-recapture: A photo-ID case study on bottlenose dolphins in Barataria Bay, Louisiana, USA.
- Haughey, R., Hunt, T., Hanf, D., Rankin, R. W., and Parra, G. J. (2020). Photographic Capture-Recapture Analysis Reveals a Large Population of Indo-Pacific Bottlenose Dolphins (*Tursiops aduncus*) With Low Site Fidelity off the North West Cape, Western Australia. *Front. Mar. Sci.*, 6.
- Henderson, E. E., Ballance, L. T., Cárdenas-Hinojosa, G., Barlow, J., DeAngelis, A. I., Martínez-Aguilar, S., Hayslip, C., Pusser, L. T., Segovia, M. M., Baker, C. S., Steel, D., Huerta-Patiño, R., Paredes, L. M. E., Brownell Jr, R. L., and Pitman, R. L. (2025). First At-Sea Identifications of Ginkgo-Toothed Beaked Whale (*Mesoplodon ginkgodens*): Acoustics, Genetics, and Biological Observations Off Baja California, México. *Marine Mammal Science*, page e70052.
- Hin, V., de Roos, A. M., Benoit-Bird, K. J., Claridge, D. E., DiMarzio, N., Durban, J. W., Falcone, E. A., Jacobson, E. K., Jones-Todd, C. M., Pirotta, E., Schorr, G. S., Thomas, L., Watwood, S., and Harwood, J. (2023). Using individual-based bioenergetic models to predict the aggregate effects of disturbance on populations: A case study with beaked whales and Navy sonar. *PLOS ONE*, 18(8):e0290819.
- Hooker, S. K., De Soto, N. A., Baird, R. W., Carroll, E. L., Claridge, D., Feyrer, L., Miller, P. J., Onoufriou, A., Schorr, G., Siegal, E., and Whitehead, H. (2019). Future directions in research on beaked whales. *Frontiers in Marine Science*, 5.
- Huggins, R. M. (1989). On the Statistical Analysis of Capture Experiments. *Biometrika*, 76(1):133–140.
- Hwang, W.-H. and Chao, A. (2002). Continuous-Time Capture-Recapture Models with Covariates. *Statistica Sinica*, 12(4):1115–1131.
- Jarvis, S. M., Morrissey, R. P., Moretti, D. J., DiMarzio, N. A., and Shaffer, J. A. (2014). Marine Mammal Monitoring on Navy Ranges (M3R): A toolset for automated detection, localization, and monitoring of marine mammals in open ocean environments. *Marine Technology Society Journal*, 48(1):5–20.
- Johnson, M., Madsen, P. T., Zimmer, W. M. X., de Soto, N. A., and Tyack, P. L. (2004). Beaked whales echolocate on prey. *Proceedings of the Royal Society of London B: Biological Sciences*, 271(Suppl 6):S383–S386.

- Jolly, G. M. (1965). Explicit Estimates from Capture–Recapture Data with Both Death and Immigration–Stochastic Model. *Biometrika*, 52(1/2):225–247.
- Jones-Todd, C. M., Pirotta, E., Durban, J. W., Claridge, D. E., Baird, R. W., Falcone, E. A., Schorr, G. S., Watwood, S., and Thomas, L. (2022). Discrete-space continuous-time models of marine mammal exposure to Navy sonar. *Ecological Applications*, 32(1).
- Joy, R., Schick, R. S., Dowd, M., Margolina, T., Joseph, J. E., and Thomas, L. (2022). A fine-scale marine mammal movement model for assessing long-term aggregate noise exposure. *Ecological Modelling*, 464:109798.
- Kéry, M. and Schaub, M. (2012). *Bayesian Population Analysis Using WinBUGS*. Academic Press.
- King, R. and McCrea, R. (2019). Capture–Recapture Methods and Models: Estimating Population Size. In *Handbook of Statistics*, volume 40, pages 33–83. Elsevier, integrated population biology and modeling, part b edition.
- Lagerquist, B. A., Irvine, L. M., Follett, T. M., Ampela, K., Falcone, E. A., Schorr, G. S., Mate, B. R., and Palacios, D. M. (2024). Blue and fin whale residence time and occupancy in Navy training and testing areas off the U.S. West Coast. *Front. Mar. Sci.*, 11:1471310.
- Link, W. A. and Eaton, M. J. (2012). On thinning of chains in MCMC. *Methods in Ecology and Evolution*, 3(1):112–115.
- Macleod, COLIN., Perrin, W., Pitman, R., Barlow, J., Ballance, LISA., D Amico, ANGELA., Gerrodette, T., Joyce, G., Mullin, K., and Palka, D. (2005). Known and inferred distributions of beaked whale species (Cetacea: Ziphiidae). *Journal of Cetacean Research and Management*, 7(3):271.
- Madon, B., Garrigue, C., Pradel, R., and Gimenez, O. (2013). Transience in the humpback whale population of New Caledonia and implications for abundance estimation. *Marine Mammal Science*, 29(4):669–678.
- Marques, T. A., Thomas, L., Ward, J., DiMarzio, N., and Tyack, P. L. (2009). Estimating cetacean population density using fixed passive acoustic sensors: An example with Blainville’s beaked whales. *The Journal of the Acoustical Society of America*, 125(4):1982–1994.
- McClintock, B. T. (2015). Multimark: An R package for analysis of capture–recapture data consisting of multiple “noninvasive” marks. *Ecology and Evolution*, 5(21):4920–4931.
- McClintock, B. T., Conn, P. B., Alonso, R. S., and Crooks, K. R. (2013). Integrated modeling of bilateral photo-identification data in mark–recapture analyses. *Ecology*, 94(7):1464–1471.
- McClintock, B. T., London, J. M., Cameron, M. F., and Boveng, P. L. (2015). Modelling animal movement using the Argos satellite telemetry location error ellipse. *Methods in Ecology and Evolution*, 6(3):266–277.
- McLellan, W. A., McAlarney, R. J., Cummings, E. W., Read, A. J., Paxton, C. G. M., Bell, J. T., and Pabst, D. A. (2018). Distribution and abundance of beaked whales (Family Ziphiidae) off Cape Hatteras, North Carolina, U.S.A. *Marine Mammal Science*, 34(4):997–1017.
- Moore, J. E. and Barlow, J. P. (2013). Declining abundance of beaked whales (Family Ziphiidae) in the California Current large marine ecosystem. *PLoS ONE*, 8(1):e52770.

- Moore, M. J., Mitchell, G. H., Rowles, T. K., and Early, G. (2020). Dead Cetacean? Beach, bloat, float, sink. *Front. Mar. Sci.*, 7:333.
- Moretti, D., Di Marzio, N., Thomas, L., Harwood, J., Schorr, G. S., and Falcone, E. A. (2018). A Population Consequences of Acoustic Disturbance Model for Cuvier's beaked whales (*Ziphius cavirostris*) in Southern California. Technical Report N0001415WX01677 / N000141512191 / N000141512899, Report prepared for the Office of Naval Research.
- Moretti, D., Marques, T., Thomas, L., DiMarzio, N., Dilley, A., Morrissey, R., McCarthy, E., Ward, J., and Jarvis, S. (2010). A dive counting density estimation method for Blainville's beaked whale (*Mesoplodon densirostris*) using a bottom-mounted hydrophone field as applied to a mid-frequency active (MFA) sonar operation. *Applied Acoustics*, 71(11):1036–1042.
- Murray, D. L. and Sandercock, B. K. (2019). *Population Ecology in Practice*. Wiley-Blackwell, 1 edition.
- New, L. F., Moretti, D. J., Hooker, S. K., Costa, D. P., and Simmons, S. E. (2013). Using energetic models to investigate the survival and reproduction of beaked whales (family Ziphiidae). *PLoS ONE*, 8(7):e68725.
- Onoufriou, A. B., Gaggiotti, O. E., Aguilar de Soto, N., McCarthy, M. L., Morin, P. A., Rosso, M., Dalebout, M., Davison, N., Baird, R. W., Baker, C. S., Berrow, S., Brownlow, A., Burns, D., Caurant, F., Claridge, D., Constantine, R., Demaret, F., Dreyer, S., uras, M., Durban, J. W., Frantzis, A., Freitas, L., Genty, G., Galov, A., Hansen, S. S., Kitchener, A. C., Martin, V., Mignucci-Giannoni, A. A., Montano, V., Moulins, A., Olavarria, C., Poole, M. M., Reyes Suárez, C., Rogan, E., Ryan, C., Schiavi, A., Tepschich, P., Urban R., J., West, K., Olsen, M. T., and Carroll, E. L. (2022). Biogeography in the deep: Hierarchical population genomic structure of two beaked whale species. *Global Ecology and Conservation*, 40:e02308.
- Oro, D. and Doak, D. F. (2020). Breeding transients in capture–recapture modeling and their consequences for local population dynamics. *Sci Rep*, 10(1):15815.
- Pabst, D. A., McLellan, W. A., and Rommel, S. A. (2016). How to build a deep diver: The extreme morphology of mesoplodons. *Integrative and Comparative Biology*, 56(6):1337–1348.
- Peltier, H., Authier, M., Dabin, W., Daniel, P., Dars, C., Demaret, F., Meheust, E., Ridoux, V., Spitz, J., and Canneyt, O. V. (2025). I sink therefore I am: 20 years of tagging small cetacean carcasses in the North-East Atlantic for bycatch estimation. *Journal for Nature Conservation*, 87:127005.
- Pirotta, E., Booth, C. G., Calambokidis, J., Costa, D. P., Fahrbusch, J. A., Friedlaender, A. S., Goldbogen, J. A., Harwood, J., Hazen, E. L., New, L., Santora, J. A., Watwood, S. L., Wertman, C., and Southall, B. L. (2022a). From individual responses to population effects: Integrating a decade of multidisciplinary research on blue whales and sonar. *Animal Conservation*, page acv.12785.
- Pirotta, E., Booth, C. G., Costa, D. P., Fleishman, E., Kraus, S. D., Lusseau, D., Moretti, D., New, L. F., Schick, R. S., Schwarz, L. K., Simmons, S. E., Thomas, L., Tyack, P. L., Weise, M. J., Wells, R. S., and Harwood, J. (2018). Understanding the population consequences of disturbance. *Ecology and Evolution*.
- Pirotta, E., Thomas, L., Costa, D. P., Hall, A. J., Harris, C. M., Harwood, J., Kraus, S. D., Miller, P. J., Moore, M. J., Photopoulou, T., Rolland, R. M., Schwacke, L., Simmons, S. E., Southall, B. L., and Tyack, P. L. (2022b). Understanding the combined effects of multiple stressors: A new perspective on a longstanding challenge. *Science of The Total Environment*, 821:153322.

- Pirotta, E., Thompson, P. M., Cheney, B., Donovan, C. R., and Lusseau, D. (2015). Estimating spatial, temporal and individual variability in dolphin cumulative exposure to boat traffic using spatially explicit capture–recapture methods. *Animal Conservation*, 18(1):20–31.
- Plummer, M., Best, N., Cowles, K., and Vines, K. (2006). CODA: Convergence diagnosis and output analysis for MCMC. *R News*, 6(1):7–11.
- Podesta, M., D’Amico, A., Pavan, G., Drougas, A., Komnenou, A., and Portunato, N. (2006). A review of Cuvier’s beaked whale strandings in the Mediterranean Sea. *Journal of Cetacean Research and Management*, 7(3):251–261.
- Pradel, R. (1996). Utilization of Capture-Mark-Recapture for the Study of Recruitment and Population Growth Rate. *Biometrics*, 52(2):703–709.
- Quick, N. J., Cioffi, W. R., Shearer, J. M., Fahlman, A., and Read, A. J. (2020). Extreme diving in mammals: First estimates of behavioural aerobic dive limits in Cuvier’s beaked whales. *J Exp Biol*, 223(18):jeb222109.
- R Core Team (2025). R: A language and environment for statistical computing. R Foundation for Statistical Computing.
- Robert Brownell Jr, Barbara Taylor, and Robin Baird (2020). *Ziphius cavirostris*. *IUCN Red List of Threatened Species*, (e.T23211A50379111).
- Rogers, A. D., Lavelle, A., Baird, R. W., Bender, A., Borroni, A., Hinojasa, G. C., Cioffi, W. R., Elliott, B. W., Harms, C., Harshbarger, A. E., Jacoby, A.-M., Lienhard, K., Mantell, S., McLellan, W. A., Merrill, G., Pabst, D. A., Rittmaster, K., Rosso, M., Schorr, G., Southall, B. L., Swaim, Z. T., Tepsich, P., Thayer, V. G., Urien, K. W., Waples, D. M., Webster, D. L., Wisse, J., Wright, D. L., and Read, A. J. (2024). A call to rename *Ziphius cavirostris* the goose-beaked whale: Promoting inclusivity and diversity in marine mammalogy by re-examining common names. *Marine Mammal Science*, 40(3).
- Royle, J. Andrew., Chandler, R. B., Sollmann, Rahel., and Gardner, Beth. (2013). *Spatial Capture-Recapture*. Academic Press.
- Rushing, C. S. (2023). An ecologist’s introduction to continuous-time multi-state models for capture–recapture data. *Journal of Animal Ecology*, 92(4):936–944.
- Sasso, C. R., Braun-McNeill, J., Avens, L., and Epperly, S. P. (2006). Effects of transients on estimating survival and population growth in juvenile loggerhead turtles. *Marine Ecology Progress Series*, 324:287–292.
- Schoenbeck, C. M., Solsona-Berga, A., Franks, P. J. S., Frasier, K. E., Trickey, J. S., Aguilar, C., Schroeder, I. D., Širović, A., Bograd, S. J., Gopalakrishnan, G., and Baumann-Pickering, S. (2024). *Ziphius Cavirostris* presence relative to the vertical and temporal variability of oceanographic conditions in the Southern California Bight. *Ecology and Evolution*, 14(7):e11708.
- Schofield, M. R., Barker, R. J., and MacKenzie, D. I. (2009). Flexible hierarchical mark-recapture modeling for open populations using WinBUGS. *Environ Ecol Stat*, 16(3):369–387.
- Schorr, G. S., Falcone, E. A., Moretti, D. J., and Andrews, R. D. (2014). First long-term behavioral records from Cuvier’s beaked whales (*Ziphius cavirostris*) reveal record-breaking dives. *PLoS ONE*, 9(3).

- Schwarz, C. J. and Arnason, A. N. (1996). A General Methodology for the Analysis of Capture-Recapture Experiments in Open Populations. *Biometrics*, 52(3):860–873.
- Seber, G. A. F. (1965). A Note on the Multiple-Recapture Census. *Biometrika*, 52(1/2):249–259.
- Seber, G. A. F. and Schofield, M. R. (2019). *Capture-Recapture: Parameter Estimation for Open Animal Populations*. Statistics for Biology and Health. Springer International Publishing.
- Shearer, J. M., Quick, N. J., Cioffi, W. R., Baird, R. W., Webster, D. L., Foley, H. J., Swaim, Z. T., Waples, D. M., Bell, J. T., and Read, A. J. (2019). Diving behaviour of Cuvier's beaked whales (*Ziphius cavirostris*) off Cape Hatteras, North Carolina. *Royal Society Open Science*, 6(2).
- Siegal, E., Hooker, S. K., Isojunno, S., and Miller, P. J. O. (2022). Beaked whales and state-dependent decision-making: How does body condition affect the trade-off between foraging and predator avoidance? *Proc. R. Soc. B.*, 289(1967):20212539.
- Silva, M. A., Magalhães, S., Prieto, R., Santos, R. S., and Hammond, P. S. (2009). Estimating survival and abundance in a bottlenose dolphin population taking into account transience and temporary emigration. *Marine Ecology Progress Series*, 392:263–276.
- Somerford, T. R., Dawson, S. M., Slooten, E., Guerra, M., Childerhouse, S. J., Richter, C. F., van der Linde, M. L., and Rayment, W. J. (2022). Long-term decline in abundance of male sperm whales visiting Kaikōura, New Zealand. *Marine Mammal Science*, 38(2):606–625.
- Southall, B. L., Benoit-Bird, K. J., Moline, M. A., and Moretti, D. (2019). Quantifying deep-sea predator-prey dynamics: Implications of biological heterogeneity for beaked whale conservation. *Journal of Applied Ecology*.
- Sweeney, D. A., Schorr, G. S., Falcone, E. A., Rone, B. K., Andrews, R. D., Coates, S. N., Watwood, S. L., DeRuiter, S. L., Johnson, M. P., and Moretti, D. J. (2022). Cuvier's beaked whale foraging dives identified via machine learning using depth and triaxial acceleration. *Marine Ecology Progress Series*, 692:195–208.
- Tanner, M. A. and Wong, W. H. (1987). The Calculation of Posterior Distributions by Data Augmentation. *Journal of the American Statistical Association*, 82(398):528–540.
- Telenský, T., Storch, D., Klvaňa, P., and Reif, J. (2024). Extension of Pradel capture-recapture survival-recruitment model accounting for transients. *Methods in Ecology and Evolution*, 15(2):388–400.
- Tenan, S., Moulins, A., Tepsich, P., Bocconcini, A., Verga, A., Ballardini, M., Nani, B., Papi, D., Motta, G., Aguilar, A. S., and Rosso, M. (2023). Immigration as the main driver of population dynamics in a cryptic cetacean. *Ecology and Evolution*, 13(2):e9806.
- Trickey, J. S., Cárdenas-Hinojosa, G., Rojas-Bracho, L., Schorr, G. S., Rone, B. K., Hidalgo-Pla, E., Rice, A., and Baumann-Pickering, S. (2022). Ultrasonic antifouling devices negatively impact Cuvier's beaked whales near Guadalupe Island, México. *Commun Biol*, 5(1):1005.
- Tyack, P. L., Johnson, M., Soto, N. A., Sturlese, A., and Madsen, P. T. (2006). Extreme diving of beaked whales. *Journal of Experimental Biology*, 209(21):4238–4253.

- Tyack, P. L., Thomas, L., Costa, D. P., Hall, A. J., Harris, C. M., Harwood, J., Kraus, S. D., Miller, P. J. O., Moore, M., Photopoulou, T., Pirotta, E., Rolland, R. M., Schwacke, L. H., Simmons, S. E., and Southall, B. L. (2022). Managing the effects of multiple stressors on wildlife populations in their ecosystems: Developing a cumulative risk approach. *Proceedings of the Royal Society B: Biological Sciences*, 289(1987):20222058.
- Visser, F., Merten, V. J., Bayer, T., Oudejans, M. G., de Jonge, D. S. W., Puebla, O., Reusch, T. B. H., Fuss, J., and Hoving, H. J. T. (2021). Deep-sea predator niche segregation revealed by combined cetacean biologging and eDNA analysis of cephalopod prey. *Sci. Adv.*, 7(14):eabf5908.
- Viterbi, A. (1967). Error bounds for convolutional codes and an asymptotically optimum decoding algorithm. *IEEE Transactions on Information Theory*, 13(2):260–269.
- West, K., Walker, W., Baird, R., Mead, J., and Collins, P. (2017). Diet of Cuvier’s beaked whales (*Ziphius cavirostris*) from the North Pacific and a comparison with their diet world-wide. *Marine Ecology Progress Series*, 574:227–242.
- Wiggins, S. M., Thayre, B. J., Trickey, J. S., Baumann-Pickering, S., Širović, A., Roch, M. A., and Hildebrand, J. A. (2018). Summary of five years of ambient and anthropogenic sound in the SOCAL Range Complex 2012 - 2017. Marine Physical Laboratory Technical Memorandum 625, Scripps Institution of Oceanography, University of California San Diego, La Jolla, California.
- Williams, R., Vikingsson, G. A., Gislason, A., Lockyer, C., New, L., Thomas, L., and Hammond, P. S. (2013). Evidence for density-dependent changes in body condition and pregnancy rate of North Atlantic fin whales over four decades of varying environmental conditions. *ICES Journal of Marine Science*, 70(6):1273–1280.
- Zimmer, W. M. X., Johnson, M. P., Madsen, P. T., and Tyack, P. L. (2005). Echolocation clicks of free-ranging Cuvier’s beaked whales (*Ziphius cavirostris*). *The Journal of the Acoustical Society of America*, 117(6):3919.